Department of Earth Sciences

Durham University

Conference 2016

7th June

Durham University

AHGS
Arthur Holmes Geological Society

Contents

A welcome from Colin Macpherson, Head of Department

I am delighted to welcome you to the fourth Department of Earth Sciences Conference, which I am sure will be just as successful as our previous conferences. This is a unique opportunity for the Department's undergraduate and postgraduate students, postdoctoral researchers and academic staff to share the results of their work.

Level 4 undergraduates will be completing their summative assessment today by giving talks about their research projects in TR3 (ES230). Poster presentations in TR1&2 (ES228 and 229) will showcase research and coursework that has been conducted by other groups in the Department. Please take the opportunity to listen to as many talks and see as many posters as you can. It is a fantastic opportunity to learn about the work that goes on in the Department.

I would like to extend a warm welcome and the Department's thanks to our sponsors and industrial partners, ERC Equipoise and CGG, for supporting this conference.

I hope you enjoy the Conference today and, most importantly, learn about the new and exciting work going on throughout the Department. Please remember to join us to enjoy refreshments in TR1&2 at 3.30pm when we present prizes for the best talks and posters.

Best wishes,

Col

A Brief History of Earth Sciences at Durham

Aspects of the Geological Sciences have been taught at Durham University since its founding, but it was not until 1924 that the Geology Department was created, with Dr (later Professor) Arthur Holmes appointed as its head. Holmes developed a strong department, which produced a succession of distinguished professional geologists. Holmes left the department in 1943, shortly before the publication of his groundbreaking textbook 'Principles of Physical Geology'. Prof. Lawrence Wager was appointed Holmes' successor, and oversaw growth of the department, recruiting Dr David Vincent (Geochemistry) and Dr Fred Stewart (Petrology), both of whom were later elected FRS.

The department in its modern form began with the appointment of Prof. Kingsley Dunham FRS as Head in 1950. Dunham brought huge energy and vision to the role, overseeing a dramatic expansion in staff numbers. The Rookhope Borehole Project was perhaps the stand-out scientific achievement of this period, and marked the rise of Geophysics in the department, led by Prof. Martin Bott FRS. Prof. Malcolm Brown FRS arrived in 1967, and shared HoD duties with Prof. Bott for the next twelve years; petrological, mineralogical and geochemical analysis of moon rocks, returned by the Apollo missions, was a highlight of this period, and laid the foundations for the department's pre-eminent status as a centre for Geochemistry. In 2003, we became the Department of Earth Sciences, and moved to our current home – the Arthur Holmes Building – which includes state-of-the-art laboratory facilities, and purpose-built teaching rooms. The department now comprises 31 academic staff, 30 research staff, 70 PhD students and around 250 undergraduates, and is known internationally as one of the top-rated Earth Science departments in the country.

Conference Timetable

09:15 – 10:30	Oral presentations	TR 3
10:30 – 11:00	Coffee break	TR 1 / 2
11:00 – 12:30	Oral presentations	TR 3
12:30 – 14:00	Poster session 1 & buffet lunch	TR 1 / 2
14:00 – 15:30	Oral presentations	TR 3
15:30 – 17:00	Poster session 2 & evening drinks	TR 1 / 2
16:00	Awards ceremony	TR 1 / 2
17:00	Close	

Department of Earth Sciences, Floor Plan

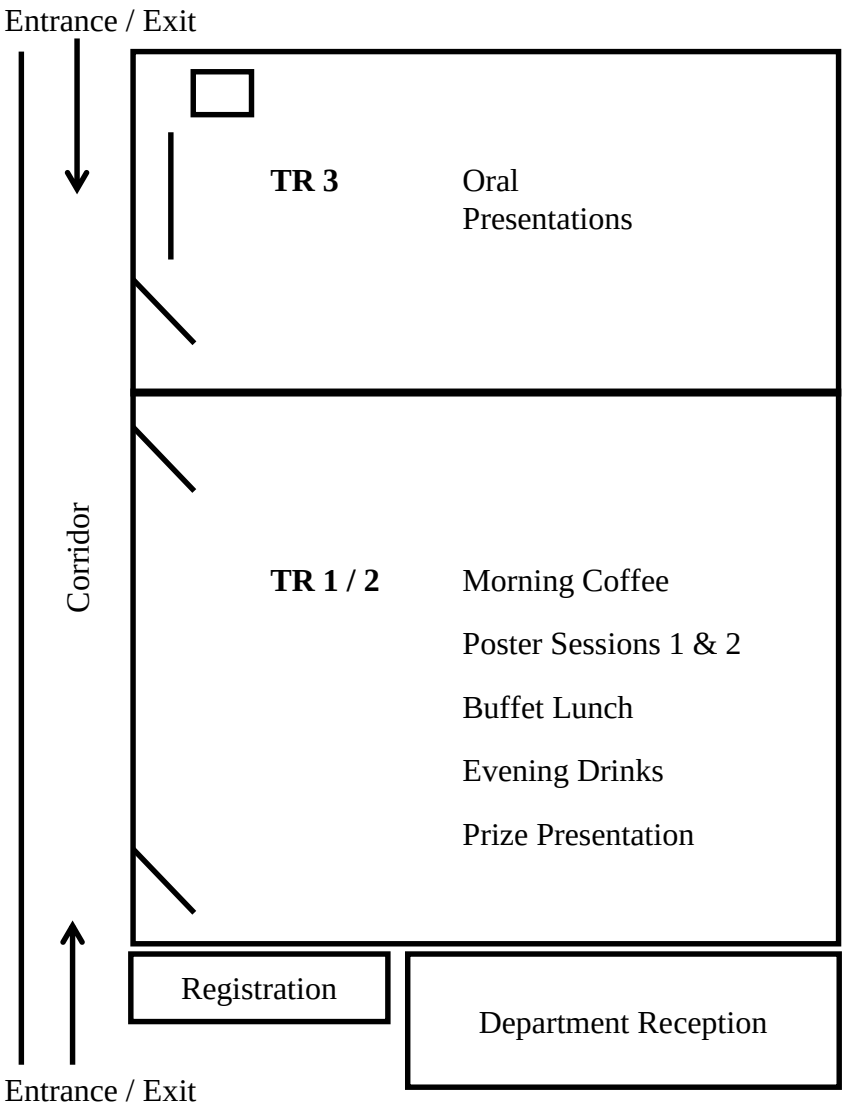

Conference Logistics

- **Registration:** From 9am outside TR1. Once you have registered you can come and go as you please throughout the day.

- **Oral presentations**: To listen to the oral presentations, PLEASE ONLY ENTER TR3 AT THE BEGINNING OF A SESSION. Please do not interrupt the oral presentations as they are being assessed. PLEASE DO NOT ENTER/LEAVE IN BETWEEN TALKS!

- **Poster presentations**: Please stand by your posters at the following times:

    - POSTER SESSION 1 (LUNCH): Staff and Postdoctoral Fellows/RAs.
    - POSTER SESSION 2 (AFTERNOON): PhD students and Undergraduates.

- **Poster setup**: Please put up your posters BEFORE the first coffee break (10.30 am).

Awards

The following awards have been kindly sponsored by the Department for the conference:

Two poster awards (1 undergraduate and 1 postgraduate): Vouchers for an outdoor shop (£50 per award)

Two awards for the best Level 4 oral presentations: Vouchers for an outdoor shop (£50 per award)

These shall be awarded by a panel consisting of AHGS representatives. Awards will be presented at 16:00 in TR1/2 – make sure you're there!

Industry Exhibition

CGG. Geoscience company providing leading geological, geophysical and reservoir capabilities to its broad base of customers primarily from the global oil and gas industry.

Geospatial Research Limited. GRL delivers integrated geoscience solutions from fieldwork, satellite and sub-surface data, primarily for the worldwide energy industry.

Durham Uni Careers, Employability and Enterprise Centre. CEEC provides a wide range of services to both students and departments, from its core functions of providing careers information, advice and guidance to students and graduates to promoting employability issues within the University.

Message from the organisers

Thank you for attending today's event! If you would like to volunteer to help organise the conference next year, or have any suggestions on how to improve the event in future, please contact claire.horwell@dur.ac.uk

2016 Conference Organising Committee:

Claire Horwell

Ryan Northam

Sasha Warren

Emma Gregory

Dean Wilson

Cat Moody

Oral Presentations

09:15	**Saw, A.S.**	Probing the Molecular-Scale Interactions between Oil and Alumina Face of Kaolinite by Means of Atomic Force Microscopy (AFM) and Chemical Force Microscopy (CFM)
09:30	**Thorogood, W.K.**	Petroleum Migration Modelling in the Offshore Barreirinhas Basin, Brazil
09:45	**Volikas, M.P.**	CO_2 Storage Potential of the Rotliegend gas fields in the Southern North Sea
10:00	**Brooksbank, H.**	Using Atomic Force Microscopy on Kaolinite to Investigate Low-Salinity Enhanced Oil Recovery
10:15	**Phillips, J.R.**	Evaluating the Combustion, Thermal and Kinetic Energy Potential of Oil, Gas and Water Produced from Norwegian High Pressure/High Temperature Petroleum Systems
10:30 – 11:00		**COFFEE**
11:00	**Roze, S.L.**	Reconstructing Lower Cambrian Ecosystems
11:15	**Alderson, J.**	On the controls and dynamics of the zero flux plane in soil plant atmosphere interaction models
11:30	**Wakefield, A.**	Linking Step Changes in Phosphorus from Sewage Treatment Effluents to the Implementation of the Urban Wastewater Treatment Directive
11:45	**Davies, R.K.**	Study of fugitive emissions of methane from high-pressure gas mains pipelines of a hydrocarbon network
12:00	**Powell, E.**	An evaluation of total phosphorus and iron removal at Lamesley co-treatment wetland system
12:30 – 14:00		**Poster Session I / LUNCH**
14:00	**Kenton, A.M.**	The Influence of Subduction Zone Characteristics on Subduction Initiation, Slab Dehydration and Mantle Wedge Rheology
14:15	**Riley, D.C.**	Analysis of avalanche density data from the Vallée de la Sionne, Switzerland

14:30	**Stephen, D.T.**	Emplacement of kimberlite lava (Igwisi Hills, Tanzania)
14:45	**Malliband, C.C.**	Magmatism and Tectonics in Perunitsa and Khosedem Fossae; and Aleksota Mons: Navka Planitia; Venus
15:00	**Groves, K.**	Characterising the basement of the Rona Ridge, West of Shetland
15:15	**O'Hare, R.**	Distribution and Timing of Faulting and Folding in the Cleveland Basin
15:30 – 17:00	**Poster Session II / DRINKS**	

Probing the Molecular-Scale Interactions between Oil and Alumina Face of Kaolinite by Means of Atomic Force Microscopy (AFM) and Chemical Force Microscopy (CFM)

Saw, A.S. **TR3** 09:15

The presence of clay minerals, in particular kaolinite plays an important role in facilitating low salinity enhanced oil recovery (LSEOR) in sandstone reservoirs. Unfortunately, successful LSEOR tests conducted on these kaolinite surfaces often rely on the assumption that they carry a permanent negative charge. Our studies looked into the alumina face of kaolinite, which is believed to have different surface charges depending on solution pH. We observed that adding low salinity brine solutions alone do not result in a decrease in adhesion, and that cation type, polar functional groups and pH were also the contributing factors. Low salinity, high pH (>8) $CaCl_2$ solutions were observed to decrease carboxylic acid (-COOH) adhesion on the alumina face to a great extent due to the expansion of the double layer. Amine ($-NH_2$) groups showed a lower effect or in some cases, increased adhesion. At pH 6, low salinity brine solutions contributes lesser to the effect on adhesion whereas high salinity brine solutions decrease the adhesion significantly. The effect at high brine salinity is due to the disruption of hydrogen bonding sites essential for hydrogen bonding between the alumina face and the functional groups of oil. As adhesion is decreased in high salinity brines ($CaCl_2$ and NaCl) at pH 6, this suggests that polar molecules do not form bonds via cation bridging or ligand bonding with the alumina face. This results in an unworkable multicomponent ion exchange (MIE) mechanism and that adhesion is mainly controlled by the electric double layer effect (EDL). Surface charge of alumina face is greatly affected by pH, which controls oil molecule adhesion by increasing or reducing the electric double layer (EDL) effect with the help of low salinity cations. The disruption of hydrogen bonding sites by high concentrations of Ca^{2+} and Na^{+} ions also plays an important role in decreasing adhesion. Therefore, we conclude that the alumina face of kaolinite, in particular the variation in surface charges caused by pH should be taken into account when considering the effectiveness of kaolinite with LSEOR as the alumina face may contribute more to the overall reaction compared to what it was expected.

Petroleum Migration Modelling in the Offshore Barreirinhas Basin, Brazil

Thorogood, W.K. **TR3** 09:30

2D seismic data from the offshore section of the Barreirinhas basin, Brazil, was provided by BG Group to model the possible migration pathways of hydrocarbon in the deep offshore section of the basin. There has been very little exploration in this frontier region so the study would assist in identifying possible targets for future exploration. The 2D seismic amplitude data was used to infer different lithofacies in each 2D seismic section, which were assigned values of capillary entry pressure taken from literature values. Permedia 5000.10.0, a petroleum systems modelling software, was used to model the likely secondary migration pathways in each section. The source rock properties, geothermal gradient and pore water density were sensitivity tested to see the effect on the hydrocarbon phase and migration routes. The extent of the vertical migration is extremely sensitive to source rock properties due to a two stage secondary migration process. This is hypothesised to be a possible model artefact. The model's pore water salinity and geothermal gradient values have an effect on both the phase and migration routes. Lateral migration is a big risk in the study area, with carrier beds providing easy routes for the hydrocarbon out of the system and hindering further vertical migration. A few key localities were identified for future exploration, and it is recommended that further seismic and source rock data is acquired for future studies.

CO_2 Storage Potential of the Rotliegend gas fields in the Southern North Sea

Volikas, M.P. **TR3** 09:45

Carbon dioxide (CO_2) emissions from fossil fuels have a strong impact on the environment, with rising concentrations in the atmosphere contributing evermore to global warming and climate change. In recent years, global attention to lower CO_2 emissions has grown due to levels of CO_2 released into the atmosphere becoming too great to ignore. One of the leading solutions to lower our emissions has been through CO_2 storage in depleting hydrocarbon fields. One benefit to storing CO_2 in depleting fields is that it can be used for enhanced hydrocarbon recovery. Another benefit of using depleting fields is that the geological structures and characteristics have been thoroughly studied and analysed when exploiting these fields for their hydrocarbon. As a result, much work has been put into collecting data for depleting fields to estimate their storage potential. Depleting gas fields are preferred for CO_2 sequestering as: ultimate gas recovery is almost double that of oil, and gas is more compressible than water. For the UK, the Rotliegend gas fields in the Southern North Sea Basin form one of the main sites for gas production, and so is one of the main areas of interest for the potential sequestering of CO_2. This talk looks at production data for these fields to calculate their cumulative production volumes. The purpose of this study is to study which fields have the potential to feasibly be converted into storage sites. By calculating drainage volumes per well and estimated storage capacity from the production volumes, factors reducing the storage potential of fields are highlighted, meaning that we can find which fields have the overall best potential. Results showed that the Rotliegend gas fields have several fields with a very high potential for sequestering CO_2. However, there were also a number of larger fields that proved to not good enough to be converted for storage.

Using Atomic Force Microscopy on Kaolinite to Investigate Low-Salinity Enhanced Oil Recovery

Brooksbank, H. **TR3** 10:00

Low-salinity water-flooding is a relatively recently discovered method of enhanced oil recovery. Laboratory studies have previously observed higher oil recovery rates when using diluted injection brines in core-flooding tests. With low-salinity water-flooding showing results of up to 40% increases in recovered oil, its success has lead researchers to try and uncover the mechanism controlling the observed effect. This project will investigate the underlying mechanisms controlling the observed low-salinity effect. The research used atomic force microscopy techniques to probe the nano-scale interactions between organic functional groups and the silica phase of kaolinite crystals. During this project, various experiments were conducted involving the submersion of kaolinite crystals bound to a mica substrate in NaCl and $CaCl_2$ brines of varying concentration and pH. Functionalized AFM tips were used to measure the adhesion of organic groups to kaolinite surfaces, and how these forces fluctuated depending on solution. Results showed that pH seemed to show a more significant influence on changing adhesion than concentration. It was often observed that higher concentrations of brines created lower levels of adhesion on the kaolinite surfaces. The impact of contact time also had an impact on the strength of readings.

Evaluating the Combustion, Thermal and Kinetic Energy Potential of Oil, Gas and Water Produced from Norwegian High Pressure/High Temperature Petroleum Systems

Phillips, J.R. **TR3** 10:15

This report considers thirteen fields currently being operated on the Norwegian Continental Shelf (NCS). These were selected due to the reservoir conditions in which they are found. Four of the fields are found within the limits currently,

generally accepted in the petroleum industry as high pressure and high temperature (HPHT) conditions of 690 bar and 149°C, whilst the other nine are found within border HPHT conditions, the lower limits of which as adopted within this report are pressures of 400 bar and temperatures of 120°C. The aim of this report is to calculate and evaluate the combustion, thermal and kinetic energies from the oil, gas and water flowing from these reservoirs based on the reservoir and monthly production data collected from the Norwegian Petroleum Directorate (NPD) and/or the operators of the fields. This will enable an assessment of the viability of harnessing thermal and/or kinetic energy to be made.

The results show that the most effective method of producing energy is through combustion, producing approximately 1-10 billion MJ/month. This method is commonly 2-3 orders of magnitude greater than thermal energy. In comparison, kinetic energy is being produced at extremely low levels, at approximately 1 MJ/month. The stage at which the investigated fields are in their productive lives most probably has an impact on the level of kinetic energy produced. The fields investigated are not yet mature enough for a high water flow to exist, thus restricting the thermal and kinetic energies that may be produced. However, binary cycle power stations may be able to efficiently harness the higher amounts of thermal energy produced at some fields. Further investigation should be conducted later in the productive life of the fields, when secondary recovery mechanisms are employed, which will increase oil, gas and eventually water production.

Reconstructing Lower Cambrian Ecosystems

Roze, S.L. **TR3** 11:00

Exploration and understanding of early complex metazoans is necessary to facilitate understanding of evolution and the nature of the first animal ecosystems. In order to understand the complexities of these ecosystems, global context is essential. Therefore, four Cambrian faunas of similar ages in carbonate systems, the Burgess Shale Fauna, Sirius Passet Lagerstätte, Wheeler Formation Fauna, Utah, and Chengjang Biota, have been examined. Data for analysis was obtained from a range of papers relating to these biota, using published species lists, and by compiling species data individually from different published papers, in order to create a matrix of species. Based on these published species, multivariate analysis of all species has been undertaken. PAST (Palaeontological Statistics) software was utilised in order to undertake species diversity and multivariate analyses, namely the Simpson's Index of Diversity and Correlation. These statistics were calculated for both species and genera, to determine whether a statistical difference was present. The biogeographic distributions of the most common species from all four faunas have been determined, to examine global distribution patterns. The Wheeler Formation and Chengjiang Biota have most in common statistically, but are furthest apart palaeogeographically. In order to reconstruct these Lower Cambrian communities and understand the complexity of the ecosystems, the feeding strategy of common species was determined and investigated, in addition to multivariate analysis, to prepare simple food webs. Factors which could influence ecological complexity, such as palaeobiogeography, facies, age, depth and oxygen availability were explored, to help determine why the Wheeler Formation had the most complex ecosystem, and the Sirius Passet, the least. It is likely that the difference in ecosystem complexity is caused by a combination of oxygen availability, substrate, facies, and age of the formation. Overall, this investigation supports the hypothesis that global biodiversity was high in the mid-Cambrian, but, although many genera are globally widespread, there are significant differences between species found in different assemblages of similar ages.

On the controls and dynamics of the zero flux plane in soil plant atmosphere interaction models

Alderson, J. **TR3** 11:15

Within a column of soil, the depth at which the hydraulic gradient, and by extension flow rate, is equal to zero represents a zero-flux plane (ZFP). Given a time series of precipitation and potential evapotranspiration data, a model can be developed to study the dynamics and controls of the ZFP. While the soil-water storage, evapotranspiration rates and vertical percolation rates can be studied with the application of a soil moisture accounting procedure, this technique cannot be used to analyse the ZFP. This study uses MATLAB software to design a model to solve Richards' equation with an incorporated plant uptake model to perform such analysis. The model presented here is a single layer of homogeneous soil of uniform thickness, with a water table 2m below the base of the soil block, with the incorporation of a gravity boundary. Input rainfall and potential evapotranspiration data are taken from a gauging station monitored by the Centre of Ecology and Hydrology. In order to solve Richards' equation for seven different soil textures (at variable thicknesses, with different vegetation root spread), soil characteristics were read from the ROSETTA pedotransfer function database and used alongside the van Genuchten soil characteristics model. This enabled the model to not only study ZFP dynamics but also to compute values for actual evapotranspiration, vertical percolation rates and storage using Richards' equation. Results from the 63 numerical simulations generated here align with inherent theories regarding soil texture and moisture content. Soil texture and root zone depth have been determined to be the main controls on ZFP dynamic, with the maximum depth of ZFP increasing either as depth of root zone or sand content increases. As expected, all simulations produced fewer ZFP plots in winter months, however, a more apparent seasonal trend is found as clay or silt content increases. Vertical percolation rates are highest in sandy soils, sandy soils also provide less water for potential evaporation, while surface run-off is only exhibited in clay soils. The author acknowledges limitations with this model, appropriately addresses them and suggests areas for further research accordingly.

Linking Step Changes in Phosphorus from Sewage Treatment Effluents to the Implementation of the Urban Wastewater Treatment Directive

Wakefield, A. **TR3** 11:30

The expansion of urban development and anthropogenic activities has been associated with an upsurge in the occurrence of eutrophication. In light of this, the Urban Wastewater Treatment Directive (91/271/EEC) (UWWTD) was adopted in 1991 in an attempt to protect the environment from urban wastewater discharge. This study investigates the link between sudden step changes, observed in phosphorus (P) concentration, from wastewater treatment plant (WWTP) effluents to the implementation of the UWWTD across England. The period of interest was 1990 – 2005 and reflects the length of records available. An objective method of visual analysis was used to identify the occurrence of step changes in 1,369 WWTPs. Step properties, such as step size and step efficiency, were calculated for each step. Correlative statistical methods were used to determine the relationship between timing of step change, permit change and calculated step properties. A significant strong relationship was found between step date and permit change date, alongside a moderate relationship between step timing and step efficiency. Changes in permit were categorised by changes to the consented determinands. The most common changes to consented determinands were the addition of iron and phosphorus. One-way ANOVAs were used to compare the means of step properties between the categories of determinand change. There were differences

observed in the means of step size and step efficiency between categories of; Fe and P addition, Fe addition only and no addition of Fe or P, significant to a 90 % confidence level. The addition of both Fe and P to consented determinands resulted in the highest mean step size and step efficiency. This was attributed to changes in the function of WWTPs, most likely to meet the requirements outlined by the UWWTD. The requirement for frequent well documented monitoring of water quality is highlighted by this study.

Study of fugitive emissions of methane from high-pressure gas mains pipelines of a hydrocarbon network

Davies, R.K. **TR3** 11:45

This study considers the greenhouse gas (GHG) footprint of conventional hydrocarbon production by considering the fugitive methane (CH_4) emissions from high-pressure gas pipelines from two areas in North Yorkshire, UK: Pickering and Malton. To fully understand the possible future use of unconventional natural gas, current conventional gas use needs to be quantified. Direct soil gas measurements were taken along two natural gas pipelines, commissioned 45 and 21 years ago respectively. The sites were surveyed for elevated concentrations of soil gas CH_4 at the surface assessed relative to a nearby control site of the same soil type and land use. This study found that of 631 survey line measurements analysed in Pickering, 307 had a surface soil gas CH_4 greater than their respective control, with 324 having lower. In Malton, 196 survey line measurements were analysed; 85 had surface soil gas CH_4 greater than their respective control, with 107 having lower. The geometric mean CH_4 flux measured from the Pickering pipeline was 76.8 ± 2.04 kg CH_4/leak/yr with the largest leak measured giving a flux of 564 kg CH_4/leak/yr. In Malton, the geometric mean CH_4 flux was 43.1 ± 3.21 kg CH_4/leak/yr with the largest leak measured producing a flux of 168 kg CH_4/leak/yr. The smallest leak detectable was 3% above ambient (1.03 relative concentration) with any leaks below 3% above ambient assumed ambient. The number of leaks detected along the pipelines correlate to the estimated length of pipe joints, inferring that there are constant fugitive CH_4 emissions from these joints. The source of CH_4 and route from pipeline to surface is unknown. The fugitive emissions measured along the Pickering pipeline, when scaled up to the UK's National Transmission System pipeline length of 7600 km gives a fugitive CH_4 flux of 62.6 kt CH_4/yr with a CO_2 equivalent of 1570 kt CO_{2eq}/yr. Although these fugitive emissions are unaccounted for in many greenhouse gas emission estimates, it is instructive to compare with agricultural use, where the same CH_4 flux is emitted by less than a quarter of the UK's sheep population.

An evaluation of total phosphorus and iron removal at Lamesley co-treatment wetland system

Powell, E. **TR3** 12:00

In 2005 the first full-scale co-treatment wetland system in the world was commissioned near Lamesley, North-East England. The wetlands receive two large inflows of secondary sewage effluent (~100 L/s) and mine water (~300 L/s). This report evaluates total phosphorus and iron removal 10 years after commission.

The evaluation of historical data supplied by the Northumbrian Water Ltd. (NWL) and the Coal Authority (CA), from 2007 until 2015 reveals high removal rates for total phosphorus and iron. Average total phosphorus treatment efficiency in the north and south wetland systems is 78% and 79%, respectively. The average iron treatment efficiency is greater: 87% and 93% for the north and south wetland systems. Total phosphorus removal is comparable in the north and south wetland systems, despite an additional wetland cell in the south wetland system. However, conflicting results presented in this study make it difficult to establish whether the additional wetland cell in the south wetland system has a significant impact on iron treatment efficiency.

This research includes new water quality data collected throughout the entire wetland system in the summer of 2015. Using this data, we are able to identify how many wetland cells provide significant removal of total phosphorus and iron. Pairwise comparisons confirm that all significant removal occurs in the initial two wetland cells. This reiterates findings from the historical data and proves that co-treatment wetland systems are an effective, low cost method of removing total phosphorus and iron from sewage effluent and mine water.

The Influence of Subduction Zone Characteristics on Subduction Initiation, Slab Dehydration and Mantle Wedge Rheology

Kenton, A.M. **TR3** 14:00

Subduction zones are key tectonic processes, responsible for the movement of water throughout the lithosphere and asthenosphere. Despite this, their initiation is poorly understood. Modelling shows a new subduction zone to go through initial descent and slab dehydration, followed by volatile and melt ascent through the mantle wedge, before reaching a steady state. From 2-D modelling of subduction zones with varying values of slab velocity, slab age and overriding plate thickness, it was found that velocity has the greatest influence on the time taken after initiation for dehydration to occur, the depth range of dehydration and melt production, and the time taken for water to rise through the mantle wedge. A faster slab causes these events to happen sooner and over a larger depth range. An older slab results in a greater depth range of water and melt, but only minimally affects the timings of dehydration or water ascension. A thinner plate results in quicker water movement in the mantle wedge and shallower dehydration, but has little impact on the start of dehydration. There is potential for age and thickness to affect where dehydration occurs within the slab and the composition of melt produced for associated volcanism. Faster slabs or thinner overriding plates encourage earlier lithospheric thinning, weakening of the crust, mantle wedge corner flow and large-scale arc volcanism, after initiation. The thermal regime is shown to be warmer in young slabs, supporting adakite production at the base of the lithosphere. Modelling of the Philippine Trench shows this fast moving slab to reach equilibrium ~5 Myr after initiation, with volcanism after 2 – 2.7 Myr. Adakites are present in the region, despite the slab being conventionally too old for production. Significant melt is seen at 35 – 50 km depth, suggesting production from stalled melt at the base of the lithosphere.

Analysis of avalanche density data from the Vallée de la Sionne, Switzerland

Riley, D.C. **TR3** 14:15

Detailed analysis of powder snow avalanches is required to quantify their hazard, which is necessary to mitigate risk as development increases in avalanche-prone regions. To this end avalanche test sites, such as the Vallée de la Sionne, have been established to allow measurement of multiple parameters in full scale flows.

This paper presents avalanche time-density profiles for ten events which occurred at the Vallée de la Sionne test site between 2006 and 2012. Measurements are provided from apparatus mounted on a 20 m pylon in the avalanche path. These are analysed to describe structural and compositional variations within the flows. Results of density analysis are compared to those of other data.

Five distinct flow regimes are defined, although not all are present in every event. These fit with existing models of avalanche structure. High velocity avalanche heads are characterised by short duration profiles showing increasing density. These are usually followed by energetic clouds, whose profiles are predominantly low density, with a small proportion of denser material. This material is either entrained compacted deposits, or particle clusters formed from aggregation in the cloud. Dense flow phases persist for long durations due to their low velocity. They show an

elevated mean density indicative of compacted material. Distinct tail sections are rarely seen due to their low energy, limiting detectable material. A powder cloud suspension is seen on most records, characterised by small fluctuations at low density. This is caused by a turbulent suspension of fine material and entrained air above the main flow. Wet material is found infrequently; where it is entrained it forms slow moving dense phases, confined close to the ground. These are indicated by long duration chaotic signals. This work provides detailed analysis of flow regimes within mixed powder snow avalanches, which can be used in avalanche modelling and management.

Emplacement of kimberlite lava (Igwisi Hills, Tanzania)

Stephen, D.T. **TR3** 14:30

The Igwisi Hills volcanoes represent the only kimberlite to show effusively erupted lava still to be preserved at the surface. Lava from the North East volcano is observed to be calcite-rich and contain a high abundance of olivine, hence it has been classified as a calcitic kimberlite with a composition tending towards carbonatite. Olivine crystals occur throughout the lava in two distinct size classes, xenocrysts and phenocrysts. The size, shape and distribution of these crystals have been investigated via the use of 2-D textural analysis. Petrographic and physical observations have also been used to ultimately build up an interpretation of lava's ascent and emplacement. Photographs from Igwisi Hills, hand specimens, thin sections and scanning electron microscope imagery provided a range of scales to observe the deposit. Rounded elliptical olivine xenocrysts make up a xenocryst-rich layer towards the bottom of the flow. They experience strong crystal alignment, which is also apparent in euhedral phenocrysts and elongated calcite laths. Crystallisation of the groundmass occurred prior to eruption due to degassing of the volatile-rich magma, this subsequently increased the viscosity of the flow and negated gravity settling of olivine xenocrysts. Low lava effusion rates are deemed to control the nature of the propagating lava, likely forming pahoehoe lobes that inflated to give the present day >2 metre section seen at Igwisi Hills. During lava effusion composition of the melt is believed to have changed from xenocryst-rich to xenocryst-poor. Xenocrystic olivine's smooth elliptical shape arose from turbulent ascent from the mantle, whereas phenocrysts crystallised directly from the kimberlite melt.

Magmatism and Tectonics in Perunitsa and Khosedem Fossae; and Aleksota Mons: Navka Planitia; Venus

Malliband, C.C. **TR3** 14:45

Venus is a tectonically and volcanically active planet and processes driving tectonics and magmatism are not fully understood. This talk presents new tectono-magmatic feature mapping of the area around Perunitsa and Khosedem Fossae, including the Venera 13 landing ellipse. From this mapping a new history of the area has been determined. The history has incorporated application of the 2 point azimuth method for determining anisotropy in point data. The 2 point azimuth method is used to determine the age and influence of tectonism on a shield field, demonstrating the usefulness of the method to define the age of features that otherwise would be ambiguous in timing. This has shown vents in a shield field grew under the influence of local extensional faulting. This study can be utilised in further understanding the history of Perunitsa and Khosedem Fossae, and magmatism patterns elsewhere on Venus.

Characterising the basement of the Rona Ridge, West of Shetland

Groves, K. **TR3** 15:00

Naturally fractured, impermeable crystalline rocks have been recognised as a petroleum reservoir, with oil hosted in fractures, including in the Rona Ridge of the Faroe-Shetland basin. Basement cores 205/21-1a, 206/7a-2, 206/12-1, 206/9-2 and 208/27-2 from the region have been studied. The

Rona Ridge basement is composed of quartzofeldspathic gneiss and foliated granite. Microstructural analysis has shown down temperature ductile metamorphism with overprinting relationships, from lower granulite to greenschist facies and brittle deformation. No widespread Laxfordian deformation is present, showing a different tectonothermal history to the onshore Lewisian Gneiss Complex, suggesting this is part of the Faroe-Shetland Block. Pervasive fracture sets, with epidote, haematite, quartz, calcite and pyrite fracture fill are present. Sedimentary fill, cockade breccia and vuggy mineral fill are found to be associated with oil-bearing fractures. These formed near to the surface at slow rates of mineralisation. The presence of oil in the fractures is proposed to have shut down mineralisation, inferring that mineralisation occurred in the Late Cretaceous Period at the time of oil charge.

Distribution and Timing of Faulting and Folding in the Cleveland Basin

O'Hare, R. **TR3** 15:15

The Cleveland Basin is part of the Southern North Sea Basin complex, in the northeast of England. The basin has been inverted. This report will investigate deformation of the basin, specifically focusing on the timing and distribution of the folding and faulting. The 2D seismic data available on the UK onshore geophysical library website has been used to analyse the deformation. Two approaches have been used, firstly, the seismic profiles were studied manually to search for structures trending both N-S and E-W. Growth folding and faulting were of key interest to ascertain the timing of the deformation. Once this was completed, a 3D model of the Penarth horizon was made in Arc. The seismic profiles were used to mark the reflector of the top of the Penarth Group to create a 3D layer across the entire basin. The deformation in the northern part of the basin is fold dominated. The small E-W folds have amplitudes ~100 m and wavelengths of 2 km. The N-S folds have amplitudes of ~50 m and wavelengths of ~ 1.2 km. The E-W folding was formed during the Cenozoic by Alpine related compressional forces. The N-S folding may have been caused by compression related to the opening of the North Atlantic Ocean. The deformation in the south part of the basin is fault dominated. A graben structure can be observed between the Vale of Pickering and Flamborough Head fault zones. The E-W and N-S trending folding in the south is gentler, with longer wavelengths than in the north. From observation of growth faulting, the extensional deformation of the fault zones occurred in the upper Jurassic and Cretaceous as well as the Cenozoic. The failure of the basin hinge zone between the rapidly subsiding basin to the north and the stable Market Weighton Block to the south may have caused the extension.

Poster Presentations

Level 2 Undergraduate

01	**Aldiss, G.**	What is the seismically induced tsunami risk to California's nuclear power stations, and how many people are at risk from an associated nuclear reactor meltdown?
02	**Elliot, B.**	The Structural and Tectonic History of Scremerston, North Northumberland
03	**Jones, T.L.**	Application of GIS in Production of a Regional Landslide Susceptibility Map, California
04	**Rothwell, N.**	The Structure and tectonic history of the Scremerston region, Northumberland
05	**Scott, J.M.A.**	Investigating the geological and tectonic history of Scremerston, Northumberland
06	**Whitford, A.C.**	The structure and tectonic history of the Scremerston region, Northumberland

Level 3 Undergraduate

07	**Alshafai, R. & Alhamad, A.**	Using sediment structure to understand ocean plate tectonics in the Panama Basin
08	**Desouza E. et al.**	Atomic force microscopy application in mineral-solution interface geochemistry. The case of gypsum and Hashemite crystal growth and the influence of Cu in the dissolution of aragonite

MSc Student

09	**Erdogan, A.R.**	Interpretation of clay swelling via non-contact linear displacement meter
10	**Goddard, C. et al.**	Earthquakes, elevations and the construction of continental plateaux

PhD Student

11	**Abdulkareem, L.**	Geophysical evidence for fluid flow in the Laminaria High, Bonaparte basin, Northwest shelf of Australia
12	**Andikagumi, H.**	The Distribution and Controls of Mariana Arc Volcanoes Location
13	**Atar, E. et al.**	Spatial and Temporal Heterogeneities of the Kimmeridge Clay Formation

14	**Cornet, J. et al.**	Modelling trace element behaviour during dehydration and melting processes. A coupled Thermodynamical/numerical approach
15	**Freeburn, R.J. et al.**	Constraining Slab Breakoff Induced Magmatism through Numerical Modelling
16	**Gaiani, I.**	Quantitative controls of pore systems in carbonate-rich shales: the Eagle Ford example
17	**Ge, X. et al.**	Apatite fission track and Re-Os geochronology of the Xuefeng Uplift, China: Temporal implications for dry gas associated hydrocarbon systems
18	**Harbord, C. et al.**	Fault zone roughness controls slip stability
19	**Hirst, C.M. et al.**	The East Midlands Petroleum Province: A New Geothermal Prospect?
20	**Horan, K. et al.**	Rapid weathering of rock-bound organic carbon driven by mountain glaciation
21	**Kareem, R. et al.**	Insights of Berea Sandstone Wettability Alteration as A-model of Sandstone Reservoir through Contact Angle Measurements
22	**Lăpădat, A. et al.**	Seismic imaging of deformation zones associated with normal fault-related folding
23	**Leung, J.N.S. et al.**	The Effect of pH on Pesticide-Soil-Mineral Interactions: A Molecular Modelling Study of Glyphosate-Clay Interfaces
24	**Li, Y. et al.**	Fluid inclusion characteristics and molybdenite Re-Os geochronology of the Qulong porphyry copper-molybdenum deposit, Tibet
25	**Liu, J. & Selby, D.**	Rhenium-Osmium geochronology and oil-source correlation of Duvernay Petroleum System, Western Canada Sedimentary Basin: Implications on the application of Re-Os geochronometer on petroleum system
26	**Liu, Z. & Selby, D.**	Variations of $^{187}Os/^{188}Os$ through late Permian and implication for paleoenvironment, Lianyuan basin, South China
27	**Maunder, B. et al.**	The Delamination and Underplating of the Subducting Crust, and Slow Subduction
28	**Michelioudakis, D. et al.**	Bayesian uncertainty analysis for advanced seismic imaging - Application to the Mentelle Basin, Australia

29 **Murray, R. et al.** The architecture and frictional properties of faults in shale

30 **Nanne, J.A.M. et al.** Testing the late veneer hypothesis with Os stable isotopes

31 **Narayan, N.** Deep Palaeozoic Karst: Geothermal Potential In Britain

32 **Obaid, A.K. & Allen M.B.** Landscape maturity and fold growth timing in the Kirkuk Embayment of the Zagros, northern Iraq

33 **Oye O. et al.** The Significance of Fluid Pressure on Sandstone Diagenesis

34 **Phethean J.J.J.** Madagascar's escape from Africa: New fracture zone trends and geodynamic understanding from gravity data

35 **Pozzi G.** Fault lubrication at seismic slip rates due to viscous flow in nanometric gouges?

36 **Riel N. et al.** Coupled thermodynamic and two-phase flow modelling of partially melting crust

37 **Sanford O.G. et al.** Modelling Seismic Wave Propagation within Extrusive Basalt Sequences

38 **Scott E.M. et al.** Controls on the location of arc volcanoes: An Andean study

39 **Stricker S. et al.** Importance of vertical effective stress for reservoir quality; examples from the Skagerrak Formation, Central Graben, North Sea

40 **Tomašek I. et al.** Environmental and anthropogenic factors affecting the respiratory toxicity of volcanic ash *in vitro*

41 **Underwood T.** Molecular dynamic simulations of low-salinity enhanced oil recovery

42 **Wilson M.P. et al.** A global review of anthropogenic related seismicity

Postdoctoral Research Assistant

43 **Agrusta, R.** Mechanisms controlling the modes of slab sinking through the transition zone

44 **Baldini, L.M. et al.** Natural and anthropogenic forcing of North Atlantic tropical cyclone track position since 1550 A.D.

45 **Boothroyd, I.M. et al.** Assessing the fugitive emission of CH_4 via migration along fault zones – comparing shale basins to non-shale basins

46 **Castiello, G. et al.** Cayman Trough, Caribbean Sea: crustal accretion and transform margin evolution at ultra-slow spreading rates

47 **Cooper, G.F. et al.** Volatiles in arc plumbing systems: Insights from cumulate hosted melt inclusions, Lesser Antilles

48 **Erastova, V. et al.** Dehydration study of Layered Double Hydroxides intercalated with Amino Acids: insights into the Origin of Life

49 **Moody, C.S. et al.** The carbon functional group budget of a peatland

50 **Simao, N. et al.** The Origin and Evolution of Oceanic Core Complexes at 13°N on the Mid-Atlantic Ridge

51 **Zhang, L. et al.** 3D crustal structure beneath the Costa Rica Rift from seismic reflection tomography

Academic Staff

52 **Baldini, J.U.L. & Sherwin, C.M.** Using high-resolution monitoring data to identify the effects of cave and surface conditions on cave drip water hydrochemistry

53 **Dale, C. et al.** A partial late veneer for the source of 3.8 Ga Isua rocks: Evidence from highly siderophile elements and ^{182}W

54 **Dobson, K. et al.** Taking geology to the IMAX: Real-time 4D tomography for volcanology and beyond

55 **Goodarzi, M. et al.** Multi-scale Study of the Elastic Response of Organic-rich Shales

56 **Haddock, D. et al.** Two-Stage Multi-Particle Sintering of Kimberlitic Volcanic Ash

57 **Hobbs, R.W. et al.** ...and the OSCAR goes to...

58 **Humphreys, M.C.S. et al.** Constraining the evolving volatile and melt geochemistry of magma reservoirs using apatite

59 **Imber, J. et al.** Observations on gender equality within Durham's Department of Earth Sciences

60 **Imber, J. et al.** Natural hydraulic fractures and the mechanical stratigraphy of shale-dominated strata

61 **Kalnins, L.M. et al.** The East Australian, Tasmantid, and Lord Howe Volcanic Chains: Possible mechanisms behind a trio of hotspot trails

62 **Llewellin, E.W. et al.** Formation and Mainenance of a Viscous Plug in a Strombolian Volcanic Conduit

63	**Macpherson, C.G. et al.**	Arclife – upper plate stress influences the sources of Sunda Arc magma
64	**McElwaine, J.**	How to Snowboard on Mars
65	**Obradors-Prats, J. et al.**	Stresses, Porosity and Overpressure Modelling in Tectonic Regimes
66	**Wilson, M.P. et al.**	Biocides in hydraulic fracturing: A comparison to agricultural and assessment of hazard and vulnerability with respect to groundwater pollution
67	**Worrall, F. et al.**	The flux of organic matter through a peatland ecosystem – evidence from thermogravimetric analysis

What is the seismically induced tsunami risk to California's nuclear power stations, and how many people are at risk from an associated nuclear reactor meltdown?

Aldiss, G.
Level 2 Undergraduate 01

California is located on the west coast of the United States and covers an area of 423,970 km^2. California is the most populus State in the USA, with 39.14 million people and has the most populous county in the US; Los Angeles County with 10.1 million people, placing over a quarter of the States population in only 4058 $miles^2$. California lies on the Eastern perimeter of the Pacific Ring of Fire, consequentially it is vulnerable to tectonic hazards such as earthquakes associated with the San Andreas transform plate boundary between the Pacific and North American late which bisects the State. Whilst earthquake hazards are well documented there has been significantly less research into tsunami risk to California.

California has two nuclear power plants, which both lie on the State's South West coastline. Diablo Canyon Nuclear Power Plant is the most Northern and San Onofre Nuclear Generating Station the most Southern nuclear power plant. They are potentially vulnerable to tsunamis derived from continental shelf and sea floor fault systems off the central coast and in the Ventura Basin. Given their proximity to the coastline as they utilise sea water to cool their nuclear reactors.

I have produced six maps using online data to display State topography, bathymetry, seismicity, faults and plate vectors, tsunami risk and radiation exclusion zones around the nuclear power stations and population density to calculate the number of evacuees.

The Structural and Tectonic History of Scremerston, North Northumberland

Elliott, B.
Level 2 Undergraduate 02

The rocks exposed at the northern end of Cocklawburn Beach, Scremerston, North Northumberland are part of the Lower Carboniferous Limestone Group, consisting of sedimentary beds of limestones, siltstones, sandstones and coal. The structures at high water mark include some notable folds in the limestone and shale beds. As part of a Second Year Geology Structural and Tectonics course project, representative folds were analysed with a view to constraining the likely structural and tectonic history of the area. An anticlinal, asymmetric whaleback fold (one of a succession of largely parallel folds verging towards the west) and its surroundings were studied in detail. The most probable hypothesis from the study was that the fold and its neighbours are the result of local reverse fault movement, combined with wider-scale north-south trending strike-slip movement, creating a transpressional positive flower structure, with shortening perpendicular to the strike-slip zone, and simple shear motion along the lines of faulting. An alternative hypothesis of the fold being a second order structure, i.e. part of a larger, first order fold whose axial trace is situated to the west was thought unlikely due to lack of local evidence of such a system, and geometrical difficulties.

Application of GIS in Production of a Regional Landslide Susceptibility Map, California

Jones, T.L.
Level 2 Undergraduate 03

Landslides are directly responsible for $2 billion worth of damage and 25-50 deaths per year across the USA. Several studies have been carried out in the past 20 years in relation to the use of GIS

technology to predict future landslides based upon a set of manually inputted parameters. This project builds upon the research of landslide trigger factors and produces a map showing the susceptibility of one county in California, Madera, to landslides. Data on seven different factors has been indirectly obtained, computed and prepared before being inputted into an equation in the GIS programme ArcMap. The equation automatically carried out an analysis based upon a data set entered manually and an overall susceptibility map was outputted. The method has been deemed an initial success and further research is required to determine its potential for wider use across the USA and worldwide.

The Structure and tectonic history of the Scremerston region, Northumberland

Rothwell, N.
Level 2 Undergraduate 04

The aims of this project were to investigate the structural and tectonic history of the Scremerston region through field observations of fold geometry and strain measurements. Data were collected at 3 localities, and included: lithological descriptions; sketches; and linear and planar data. Measurements were taken using a measuring tape and compass clinometer. Fold geometries varied from closed to open; all were asymmetric with some verging east and some west indicating a heterogeneous strain field. Stereonet data revealed that folds were non-cylindrical, which could be caused by transpression along converging fault planes. Slickenlines within folds revealed frictional sliding, likely due to the low confining pressure and deformation within the upper brittle crust. From comparison of the original and deformed length of the fold and measuring quartz vein thicknesses, shortening and extension were calculated to be -0.2 and 0.027, respectively. Due to cleavage formation parallel to fold axial planes, the general fabric was interpreted as an S>L-tectonite with estimated strains plotting within the field of apparent flattening. The maximum principle stress is inferred to have been in an east-west direction. Asymmetry of folds suggest that strain is heterogeneous.

Investigating the geological and tectonic history of Scremerston, Northumberland

Scott, J.M.A.
Level 2 Undergraduate 05

Beds within the Yoredale cyclothem of the Alston Formation exposed at Scremerston show a number of deformational features: intense folding, jointing/fracturing and local faulting. Analysis of these features, and their relationships, allows us to quantify the finite strain experienced by the rocks, and to infer the orientations of the principal stresses. Estimates of extension and shortening, orientations of the principal stress directions, and the folding mechanism are discussed in this study, giving an insight to the Variscan orogeny, the suspected cause of deformation. From the structures present this study deduced that the folds were of type 1B, that strain was non-coaxial/rotational and that simple shearing has taken place, the presence of slickenlines supports the idea of flexural slip during folding. The region overall likely experienced compressional deformation, with a component of strike-slip deformation, or oblique compression. The number of deformation events experienced by these formations is debatable, it may numerous, or one with fluctuating values of the principle stress. The information these features yield allows simplistic reconstructions of the compressional regime experienced by these lithologies during the Variscan orogeny and the likely orientation of the finite strain ellipsoid.

The structure and tectonic history of the Scremerston region, Northumberland

Whitford, A.C.

Level 2 Undergraduate 06

A sequence of deformed Lower Carboniferous rocks exposed on the coast at Scremerston was studied in order to determine the stress and strain conditions involved in the formation of the fold structures observed there. These data could then be used to develop an interpretation of the tectonic regime of the area.

The folds observed were asymmetrical, non-cylindrical antiforms with curvilinear hinges. However, the fold to the northern end of the study area verged to the west while the other at the southern end verged to the east. A high level of mechanical anisotropy is evident between the lithological layers forming the folds and this, along with the consistent bed thickness and slickensides observed on bedding planes indicates the folds developed by a flexural slip mechanism.

Analysis of the folds and associated joint structures showed the strain which formed the folds to be heterogeneous rotational, and variable in magnitude across the region. The area experienced overall compression parallel to σ1 (E-W).

The axial plane is twisted between the two folds, and three hypotheses are proposed to explain this unusual occurrence; 1) shearing compression occurred during the folding event, 2) fault propagation folding caused by the mechanical stratigraphy preventing further propagation of a thrust fault, 3) the existence of a pair of conjugate strike slip faults beneath the two folds.

Although no definitive answer can be reached from these observations, it is thought a combination of 1 and 2 is the most likely cause of the opposing vergence.

Using sediment structure to understand ocean plate tectonics in the Panama Basin

Alshafai, R. & Alhamad, A.

Level 3 Undergraduate 07

A 2-D marine seismic survey in the Panama Basin was accomplished during the Oscar cruise in 2015. Two seismic lines were used from this survey. The first line was to determine the sedimentation history against the age of the underlying oceanic crust around ODP Site 504B. Thrusting, normal faulting and small-scale folding were observed in the section. It was concluded, because of the presence of these compressional features and also based on in-situ stress estimates at Hole 504B, that the profile had experienced compression in its early stages. Then, at some time between the lower Pleistocene and the upper Pliocene, this compression regime was inverted to extension, which is the dominant regime at present since active normal faulting was found in the section. It was also concluded that sediments thicken toward active normal faults. Moreover, The second line was aimed to map the deep structure of the Ecuador Fracture Zone. The fracture zone consists of three median ridges and a transverse ridge. A model was used to explain the origin of the observed transverse ridge as a result of flexure response due to normal faulting. The model suggests that the ridge is formed due to normal faulting resulting in a height of 800 m. However, the observed ridge is 1000 m, which suggest a further uplift was caused by another mechanism. It was suggested that the mechanism may be a diapirs intrusion of serpentinite, which is also responsible for the formation of the median ridges.

Atomic force microscopy application in mineral-solution interface geochemistry. The case of gypsum and Hashemite crystal growth and the influence of Cu in the dissolution of aragonite

Desouza, E., Round, T., Greenwell, H.C.G. & Cubillas, P.

Level 3 Undergraduate 08

Atomic force microscopy (AFM) is a widely use technique in the field of mineral-solution interface studies. This is due to its high spatial resolution in the lateral (5-10 nm) and vertical scales (below 1 Å) and because of its capability to image surfaces under solution. These capabilities allow for the study of dissolution and growth processes in-situ, thus providing quantitative kinetic data at the scale of elementary reactions. In addition, it can provide direct observations on the type of crystal growth or dissolution mechanism involved at a particular supersaturation/temperature/chemical conditions.

Here we highlight results from three, ongoing studies on mineral-solution interface geochemistry:

1. *Crystal growth of gypsum.* Studies have been performed to assess the effect of solution stoichiometry (Ca^{2+}:SO_4^{2-}) in the crystal growth rates on the {010} face. Results indicate a variation in the rates with stoichiometry as expected, but in addition, a change in the relative growth rates across different crystallographic directions has been observed. The effect of temperature in the growth rates has also been assessed by performing experiments at 25, 40 and 60°C.

2. *Inhibition of aragonite dissolution rates by Cu.* Imaging has been performed on the {110} face of single-crystal aragonite needles, under (Ca^{2+}/CO_3^{2-}) solutions slightly undersaturated in aragonite and with a Cu^{2+} concentration of 50 M.

Inhibition of aragonite dissolution rates by Cu. Imaging has been performed on the {110} face of single-crystal aragonite needles, under (Ca2+/CO32-) solutions slightly undersaturated in aragonite and with a Cu2+ concentration of 50 M.

3. *Crystal growth of hashemite ($BaCrO_4$)*. In this system we have performed experiments to assess the effect of solution stoichiometry (Ba^{2+}:CrO_4^{2-}) on growth rates. In addition, we have studied the growth of the $BaCrO_4$-$BaSO_4$ solid solution.

Crystal growth of hashemite (BaCrO4). In this system we have performed experiments to assess the effect of solution stoichiometry (Ba2+:CrO42-) on growth rates. In addition, we have studied the growth of the BaCrO4-BaSO4 solid solution.

Interpretation of clay swelling via non-contact linear displacement meter

Erdogan, A.R.

MSc Student 09

In this study, the swelling of compacted commercial bentonite clay mineral cores was investigated using a novel non-contact displacement meter with various organic solvents and salt solutions. Swelling results with organic solvents were correlated with the dielectric constant, dipole moment, surface tension and viscosity of the solvent. It was revealed that swelling rate and total swelling were proportional with dielectric constant and inversely proportional to viscosity, indicating the chemical and capillary components of swelling action, respectively. Results of swelling tests with salt solutions are discussed in the context of diffuse double layer (DDL) theory. Swelling behaviour of smectite clay minerals was found to be highly affected by cation concentration. Tests with $CaCl_2$ solutions showed that divalent cations were effective at suppressing swelling at low concentrations. At high concentrations KCl and KI solutions were more effective at inhibiting swelling owing to the lower hydration enthalpy of K^+ cations. Comparison between bentonite and illite swelling shows that, for reconstituted compacted cores, the initial

stage of clay swelling is dominated by capillary action. Then, depending on the reactivity of the clay and the medium, chemical swelling occurs. Hereby, the swelling behaviour of compacted clay cores, as used by many drilling fluid research laboratories, is highly dependent on the domination of different swelling components in different time periods as an artefact of the sample preparation and care should be taken when using ground and compacted shales to assess either reactivity of shale formations to drilling fluids or the effectiveness of swelling inhibitor systems.

Earthquakes, elevations and the construction of continental plateaux

Goddard, C., Allen, M.B., DePaula, N. & Saville, C.
MSc Student 10

It has been noted that larger thrust earthquakes (M>~5) are rare at higher elevations in continental fold-and-thrust belts. For example, the cut-off is the 1250 m elevation contour in the Zagros fold-and-thrust belt, while thrust events are rare above 3500 m in the Himalayas and other fold-and-thrust belts marginal to the Tibetan Plateau. There are various possible explanations for this phenomenon, including aspects of the critical wedge model and one interpretation which suggests higher elevation regions resist major seismogenic thrusting due to the additional gravitational potential energy (GPE) added from the increase in height.

Here we have investigated the elevation distribution of earthquake data sets for the Qilian Shan and the Zagros, to identify a relationship between elevation and earthquake magnitude. Preliminary findings show a gradual reduction of larger thrust events rather than an abrupt termination. We aim to repeat this analysis over a variety of different areas in an attempt to quantify this relationship.

We are also investigating an alternative model, where increase in height, and therefore in lithostatic load, creates a thicker zone of distributed deformation above the temperature dependent brittle-plastic transition. This could potentially suppress the ability of large earthquakes to propagate through the entire brittle crust. Future work will involve laboratory analysis to mimic the increasing conditions of confining pressure experienced by rocks as the regional elevations increase.

Geophysical evidence for fluid flow in the Laminaria High, Bonaparte basin, Northwest shelf of Australia

Abdulkareem, L., Hobbs, R.W. & Imber, J.
PhD Student 11

Seismic amplitude anomalies (“bright spots”) can result from changes in acoustic impedance caused by the presence of fluids and/or lateral changes in lithology. In this study, we have interpreted3D seismic and well log data is used to investigate the nature and causes of seismic amplitude anomalies within the shallow subsurface on the Laminaria High, NW shelf of Australia. Here, the anomalies are associated with active faults that cut the seabed. Previous studies suggest that fault reactivation and fault geometry have an important role in causing hydrocarbon leakage from a deeper reservoir and that fault bends on larger faults will influence the localization of shear strain, increasing the risk of leakage related faults. However, these studies did not examine the influence of fault growth during reactivation on fluid migration, or how post-rift and syn-rift sedimentation may have influenced fluid leakage. In our study, preliminary results suggest that not all active faults are associated with amplitude anomalies or dry/partially-filled hydrocarbon traps at depth, implying that there could be a different mechanism of formation on the Laminaria High. Specifically, these anomalies may be the result of preferential cementation, or the presence of gas trapped within sediments at or near the seabed, perhaps originating from gas generation due to biogenic activity in recently deposited sediment. Therefore, detailed

amplitude maps will be extracted from syn- and pre- faulting seismic horizons down to the top reservoir level in order to understand the extent of the high amplitude anomalies within the stratigraphic succession, that is, to reveal whether the high amplitude anomaly shown on the amplitude map of the seabed continues downward at greater depths or whether it is restricted to very shallow features near the sea bed. In addition we will undertake a fault reconstruction to investigate how the evolving fault geometry may have influenced fluid migration on the Laminaria High.

The Distribution and Controls of Mariana Arc Volcanoes Location

Andikagumi, H.
PhD Student 12

The occurrences of volcanic arcs are important to human life and society through their related natural resources and geohazard. Subsurface processes can be identified by surface features and geometry. Previous study by England et al. (2004) described the distribution of Mariana Arc Volcanoes as small circle. The same dataset of 12 volcanoes coordinate were used in small circle fitting and resulted 2.522 km misfit. Meanwhile, the same method applied to bigger dataset from Baker et al. (2008) which consisted of 37 volcanoes and resulted 8.431 km misfit. However, using Hough Transform method, better misfits of the volcanoes to its linear segment are better than the small circle fitting which are 3.098 and 3.042 km for two different possible segmentation combination. It indicates the distribution of volcanoes in Mariana Arc is in great circle pattern, instead of small circle. It is also proved by the plot of misfit of the volcanoes along the small circle datum that formed curvy regression line. Variogram and cross-variogram analysis with spacing and volume as variables explained that there is spatial correlation between volcanoes in 420 to 500 km which corresponds to the maximum length of segmentation from Hough Transform, 320 km. However, spacing and volume of the volcanoes are not strongly correlated based on bivariate analysis, except on the central segmentation where Pagan and Agrigan volcanoes located. The spacing of the volcanoes were also analysed to determine the regularity of the spacing. Based on the coefficient of variation of the volcanoes, the spacing is regularly distributed as its value verging towards zero. To prove that the volcanoes are not randomly distributed, Monte Carlo simulation were conducted and the probability of not-random distribution for 6 volcanoes along segmentation is 0.345 and for 10 volcanoes is 0.005. These not-random distributions are associated with the coefficient of variations of the normal faults at the back arc which also verging towards zero. It indicates that the distribution of volcanoes in Mariana Arc is controlled by the early development of normal faults.

Spatial and Temporal Heterogeneities of the Kimmeridge Clay Formation

Atar, E.[1], Armstrong, H.[1], Imber, J.[1], Aplin, A.[1], März, C.[2], Wagner, T.[3] & Herringshaw, L.[4]
[1]Durham University; [2]University of Leeds; [3]Heriot Watt University; [4]Univerisity of Hull
PhD Student 13

Understanding the nature and distribution of black shales is of great interest to both the petroleum industry and palaeoclimatologists. A key aim is to better understand the underlying controls on the spatial and temporal heterogeneities in shale and their distribution and thickness. A conceptual model, developed for Cretaceous OAEs and applied to the Kimmeridge Clay Formation implicates the orbital forcing of tropical climate in the development of sedimentary and geochemical heterogeneities in black shales. Recent climate modelling of the Upper Jurassic confirm the links between the location and dynamics of the atmospheric Hadley Cell and marine organic productivity. Late Jurassic Hadley Cell dynamics are poorly constrained but in

the modern setting, the strongest contrasts in seasonal to orbital-scale fluctuations in continental precipitation, weathering, and nutrient supply to the oceans, occur at the ascending and descending limbs of inner the Hadley Cell. These contrasts and the mechanisms of formation of black shales are recorded in multi-scale heterogeneities in organic carbon quality and quantity, grain size, and bulk mineralogy. Shale geochemistry and properties can therefore be used to test the hypothesis that temporal and spatial variations in black shale deposition are controlled by orbital modulation of the Hadley Cell.

This project uses a multiproxy geochemical and sedimentological approach to determine variations in shale depositional environments and properties across a latitudinal transect from mid- to high palaeolatitude. The geographical variations in these factors will allow a better understanding of the location and width of the Hadley Cell during the Upper Jurassic greenhouse climate mode.

Modelling trace element behaviour during dehydration and melting processes. A coupled Thermodynamical / numerical approach

Cornet, J., Grigorova, V., Riel, N., Bouilhol, P. & Van Hunen, J.

PhD Student 14

Our understanding of chemical differentiation processes is mostly based on the study of exposed magmatic complexes. Trace element analysis of rocks and minerals provides a quantifiable mean of understanding the process at stake during Earth's geochemical differentiation. However, the genesis and the evolution of rocks relate to a succession of complex processes that cannot be constrained only by their trace element signature, as their represent a final state of a complex process involving metamorphic and magmatic reactions and crystallisation. For example, it is well accepted that slab dehydration, partial melting of mantle wedge, emplacement of mantle-derived melt at the Moho and assimilation/storage/hybridization in the lower crust are the processes associated with crust formation. This succession of processes is narrowly linked to the variation of pressure, temperature and chemical condition experienced by different lithologies, and will impact greatly the final trace element signature of the resulting magmas. The geochemical community relies on experimentally determined Partition coefficient to better constrain these processes, but the uses and misuse of this technique is largely hampered by our poor knowledge of the different reactions taking place throughout the history of the formation of a rock.

This project intend to elaborate an extensive dataset of partition coefficient for minerals, fluids and melts, based on experimental results, and combine it with state-of-the-art numerical models that can simulate metamorphic and subsequent melting processes. As such it will offer a way to model trace element composition of fluids and melts during metamorphic and magmatic processes in a systematic and consistent way as a function of the physical characteristics of the considered process (e.g. slab devolatilisation, melt migration, crystallization)

Hence, the project will provide a key to better understand the dynamics of melt formation and differentiation in deep processes and will, therefore, propose new insights for modern and early earth crustal formation mechanisms.

Constraining Slab Breakoff Induced Magmatism through Numerical Modelling

Freeburn, R.J., van Hunen, J., Magni, V.M., Bouilhol, P. & Maunder, B.

PhD Student 15

Post-collisional magmatism is markedly different in nature and composition than pre-collisional magmas. This is widely interpreted to mark a change in the thermal structure of the system due to the loss of the oceanic slab, allowing a different

source to melt. Early modelling studies suggest that when breakoff takes place at depths shallower than the overriding lithosphere, magmatism can occur through the decompression of upwelling asthenosphere and the thermal perturbation of the overriding lithosphere. Interpretations of geochemical data, which invoke slab breakoff as a means of generating magmatism, mostly assume these shallow depths; however more recent modelling suggest that breakoff generally occurs deeper.

Here we test the extent to which slab breakoff is a viable mechanism for generating melting in post-collisional settings. We use 2D numerical models of spontaneous collision and breakoff and determine the amount of hydration and melting using pre-calculated equilibrium mineral assemblages. Our reference model shows only small amounts of post-collisional magmatism, and hence we conduct a parametric study, systematically changing parameters which are known to reduce the breakoff depth and timing. Our models show that breakoff at shallow depths can generate a transient pulse of mantle melting, through the hydration of hotter, undepleted asthenosphere flowing in from behind the detached slab. Longer-lived melting of the continental crustal can also occur in models which show significant amounts of exhumation or delamination. However, this melting is only observed for end-member models, hence suggesting that much of the magmatism observed in collisional areas is likely generated via alternative mechanisms.

Quantitative controls of pore systems in carbonate-rich shales: the Eagle Ford example

Gaiani, I.

PhD Student 16

Shales are clastic sedimentary rocks that, if found to be rich in organic matter, may generate significant quantities of gas and oil hydrocarbons. However, shales mostly present sub-nanometer to micron-scale pore sizes, impeding the flow of hydrocarbons through the system at relatively low pressures. Moreover, these shales are texturally and mineralogically heterogeneous and for a successful recovery it is crucial to achieve a quantitative understanding of the porosity system.

This project focuses on the Eagle Ford Formation, a very heterogeneous, carbonate and organic-rich shale that trends across Texas.

A set of samples of variable maturity and facies from different locations was provided by Shell, Houston. At first, the factors that influence the mineralogy and the diagenetic processes that have occurred in the samples have been interpreted by means of XRD, transmitted and reflected light optical microscopy and SEM analysis. The resulting data gave insights into the texture and the matrix pore structure with the change of thermal maturity.

As a future analysis, pore sizes and pore connectivity will be measured by means of state-of-the-art techniques such as XRCT, Gas Adsorption (He, CO_2 and N_2) and MICP. Then, which will also be the real novelty of the work, the chemistry of the surface pores will be analysed chemically by means of a combination of AFM and nano IR-spectroscopy.

The combination of the above-mentioned methods will eventually allow us to reproduce meticulously the porosity system and to predict the flow pathways and the potential hydrocarbon storage sites.

Apatite fission track and Re-Os geochronology of the Xuefeng Uplift, China: Temporal implications for dry gas associated hydrocarbon systems

Ge, X., Shen, C., Selby, D., Deng, D. & Mei, L.

PhD Student 17

Hydrocarbon evolution is extremely challenging to determine, both temporally and spatially, in complex tectonic settings. Here we investigate the western margin of the Xuefeng Uplift, China,

which records multiple and protracted tectonic and hydrocarbon generation events. This timing of initial oil generation is recorded by low maturity bitumen (Type A), which yields a Re-Os bitumen date of ~430 Ma, consistent with basin models and a ~405 Ma bitumen Rb-Sr date. In contrast, Apatite Fission Track (AFT) data yield considerably younger dates that reflect the timing and tectonic evolution of the Yanshan Orogeny from the northwest (~150 Ma) to southeast (~70 Ma). The youngest AFT date coincides with the western margin of Xuefeng Uplift, where high maturity bitumen (Type B) occurs, which yields a ~70 Ma Re-Os date. The Re-Os and AFT dates imply that both the last stage of the Yanshan Orogeny and, by inference, the cessation of dry gas generation, occurred at ~70 Ma. The Re-Os data of this study imply that the Re-Os chronometer can aid in constraining the timing of oil generation, and of secondary and/or more mature hydrocarbon processes (e.g., thermal cracking/gas generation) in hydrocarbon systems worldwide.

Fault zone roughness controls slip stability

Harbord, C., Nielsen, S., De Paula, N., & Holdsworth, B.
PhD Student 18

Fault roughness is an important control factor in the mechanical behaviour of fault zones, in particular the frictional slip stability and subsequent earthquake nucleation and propagation. However, there is little experimental quantification as to the effects of varying roughness upon rate- and state-dependent friction (RSF). Utilising a triaxial deformation apparatus and an adaptation of the direct shear methodology to simulate initially bare faults in Westerly Granite, we performed a series of velocity step friction experiments. We varied initial root mean square roughnesses (Sq) in the range $2x10^{-6}$ –$2.4x10^{-5}$ m, normal stress in the range σ_n = 30–200MPa and slip velocities between 0.1–10 µm s^{-1}. Transitions between stable and unstable sliding are observed, dependent on the parameter combination, in particular instability observed at σ_n=100-150MPa on the smoothest fault ($Sq=2x10^{-6}$m) disappears at high normal stress. Additionally, instability can develop when the ratio of fault to critical stiffness $k_f/k_c > 10$, or, alternatively, when $a - b > 0$, suggesting that bare surfaces may not strictly obey the RSF stability condition. We instead suggest that bare fault surfaces may require a different stability criterion to gouges, based on the competition between maximum supportable weak patch length, λ_c and the critical nucleation length L_c.

The East Midlands Petroleum Province: A New Geothermal Prospect?

Hirst, C.M., Gluyas, J.G. & Mathias, S.A.
PhD Student 19

Modification of existing oilfield structure could deliver a cost effective way to extend the economic life of depleted onshore oilfields without the need to produce oil. Naturally warm connate and injection water contained within these fields could be produced and used to deliver clean, cheap, non-intermittent heating. The East Midlands Petroleum Province contains over 30 fields with a production history spanning 95 years (Craig et al., 2013), and we have chosen to examine the Welton field in detail. Well data for the Welton field has been analysed to ascertain stored heat within both oil and non-oil bearing (water) strata within the field. Production rates were calculated to be 728 m^3 d^{-1} oil and 854 m^3 d^{-1} water. This figure also includes productivity of intervening largely water bearing intervals. Target formation temperature at 1500 m was determined to be 52.5°C, allowing a stored heat energy calculation to be undertaken for a range of temperature differentials. For a total depletion in formation temperature, 1.6 MW_t stored heat is available within the Welton field alone. This equates to 14,040 MWh of heat energy available for consumption by the domestic market or within commercial greenhouses.

Rapid weathering of rock-bound organic carbon driven by mountain glaciation

Horan, K., Hilton, R.G., Selby, D., Ottley, C.J., Hicks, M. & Burton, K.W.
PhD Student 20

Over millions of years, the oxidation of organic carbon contained within sedimentary rocks is one of the main sources of carbon dioxide (CO_2) to the atmosphere, yet the controls on this CO_2 emission remain poorly constrained. Here we use rhenium to track the oxidation of rock-derived organic carbon in the mountain catchments of the western Southern Alps, New Zealand, where high rates of physical erosion expose rocks to chemical weathering. We demonstrate that oxidative weathering fluxes are three times higher in glaciated catchments. Consequently, glaciated mountain catchments tip the net carbon balance during erosion and weathering from a CO_2 sink to a CO_2 source and can act as a counter-mechanism against global cooling over geological timescales.

Insights of Berea Sandstone Wettability Alteration as A-model of Sandstone Reservoir through Contact Angle Measurements

Kareem, R., Cubillas, P., Riggs, H.J., Gluyas, J., Gröcke, D.R. & Greenwell, H.C.
PhD Student 21

Enhanced oil recovery (EOR) methods target the residual ca. 50 % of crude oil, found coating the pore surfaces of sandstone reservoirs. Low salinity water flooding EOR involves the injection of waters with low salt concentrations into the reservoir. These methods, through a contested mechanism, alter the wettability of the reservoir rock and promote oil displacement. In this work, we have used environmental scanning electron microscopy (ESEM) to measure and assess the change in wettability on oil-treated detrital quartz grains from Berea sandstone and model single-crystal high-quality quartz. Crude oil, as well as a "model-oil" (decanoic acid) where used. Wettability alteration was brought by flushing the pre-treated crystals with low concentration brines (0.01M) of different composition (NaCl, CaCl2, MgCl2, and KCl). Results show that, in the case of quartz surfaces from Berea sandstone, NaCl has the greater effect in changing the wettability state from oil wet to water wet. Results are noticeably aligned with total organic carbon (TOC) data. In contrast, the model-quartz crystals do not show great changes in wettability. The variation in results is undoubtedly due to the influence of nano-mineral coatings in the sandstone's quartz crystals, as observed by high-resolution SEM. These results also highlight the importance of using natural mineral surfaces in the EOR study

Seismic imaging of deformation zones associated with normal fault-related folding

Lăpădat, A.[1], Imber, J.[1], Iacopini, D.[2] & Hobbs, R.W.[1]
[1]Durham University; [2]University of Aberdeen
PhD Student 22

Folds associated with normal faulting, which are mainly the result of fault propagation and linkage of normal fault segments, can exhibit complex deformation patterns, with multiple synthetic splay faults, reverse faults and small antithetic Riedel structures accommodating flexure of the beds. Their identification is critical in evaluating connectivity of potential hydrocarbon reservoirs and sealing capacity of faults. Previous research showed that seismic attributes can be successfully used to image complex structures and deformation distribution in submarine thrust folds.

We use seismic trace and coherency attributes, a combination of instantaneous phase, tensor discontinuity and semblance attributes to identify deformation structures at the limit of seismic resolution, which accommodate seismic scale folding associated with normal faulting from Inner Moray Firth Basin, offshore Scotland. We identify synthetic splay faults and reverse faults

adjacent to the master normal faults, which are localized in areas with highest fold amplitudes. This zone of small scale faulting is the widest in areas with highest fault throw / fold amplitude, or where a bend is present in the main fault surface.

We also explore the possibility that changes in elastic properties of the rocks due to deformation can contribute to amplitude reductions in the fault damage zones. We analyse a pre-stack time-migrated 3D seismic data-set, where seismic reflections corresponding to a regionally-continuous and homogeneous carbonate layer display a positive correlation between strain distribution and amplitude variations adjacent to the faults. Seismic amplitude values are homogeneously distributed within the undeformed area of the footwall, with a minimum deviation from a mean amplitude value calculated for each seismic line. Meanwhile, the amplitude diming zone is more pronounced (negative deviation increases) and widens within the relay zone, where sub-seismic scale faults, which accommodate bed rotation, affect, presumably, the acoustic properties of the rocks. We calculate the finite strains associated with fault displacement (using trishear kinematic models) and generate 2D synthetic seismic sections of the model, taking into account the strain-related changes in the acoustic properties of the deformed rocks. Finally, we investigate whether variations in the magnitudes of strain correlate with the magnitudes of seismic amplitude variations near the analysed faults.

The Effect of pH on Pesticide-Soil-Mineral Interactions: A Molecular Modelling Study of Glyphosate-Clay Interfaces

Leung, J.N.S., Erastova, V., Underwood, T. & Greenwell, H.C.

PhD Student 23

Glyphosate, the active ingredient in the widely used herbicide Round-up(R), has been recently identified as a potential cause of numerous health problems. The behaviour of glyphosate in the soil has been widely studied at the macroscopic level, but a molecular-level explanation is currently lacking. In this study, the effect of pH on glyphosate–clay interactions is considered using molecular dynamics simulations. The systems studied include sodium-saturated (Na-MMT) and calcium-saturated (Ca-MMT) montmorillonite solvated with both water and with 0.1 M CaCl2 solution. In the Na-MMT systems, glyphosate adsorption decreased with increasing pH. In the Ca-MMT system, glyphosate molecules were always adsorbed to the clay mineral, however, the associated adsorption mechanisms were pH dependent. In general, at very low pH levels (< 2.2) glyphosate was directly adsorbed to the clay surface via hydrogen bonding. As pH increased, glyphosate molecules were increasingly adsorbed through electrostatic interactions with surface adsorbed calcium ions. It was also found that the 0.1M CaCl2 solution enhanced glyphosate adsorption on Na-MMT as Ca2+ ions replaced the Na+ ions initially bound to the clay surface. Since the Ca-MMT surface is already saturated with Ca2+, the addition of CaCl2 solution did not have a significant effect on glyphosate adsorption. These results have important implications for the development of the retention time models and thus a more accurate transport model for the prediction of the fate of glyphosate in soil.

Fluid inclusion characteristics and molybdenite Re-Os geochronology of the Qulong porphyry copper-molybdenum deposit, Tibet

Li, Y.[1], Selby, D.[1], Feely, M.[1], Costanzo, A.[2] & Li, X.-H.[3]

[1]Durham University; [2]National University of Ireland; [3]Chinese Academy of Sciences

PhD Student 24

The Qulong porphyry copper and molybdenum deposit is located at the southwest margin of the Lhasa aTerrane and in the eastern region of the Gangdese magmatic belt. It represents China's

largest porphyry copper system, with ~2200 million tonnes of ore comprising 0.5 % Cu and 0.03 % Mo. The mineralization is associated with Miocene granodiorite, monzogranite and quartz-diorite units, which intruded into Jurassic volcanic units in a post-collisional (Indian-Asian) tectonic setting. Field observations and core logging demonstrate the alteration and mineralization at Qulong are akin to typical porphyry copper systems in subduction settings, which comprise similar magmatic-hydrothermal, potassic, propylitic and phyllic alteration assemblages. Molybdenite Re-Os geochronology confirms the relative timeframe defined by field observations and core logging and indicates that the bulk copper and molybdenum at Qulong were deposited within 350,000 years: between 16.10 ± 0.06 [0.08] (without and with decay constant uncertainty) and 15.88 ± 0.06 [0.08] Ma. This duration for mineralization is in direct contrast to a long-lived intrusive episode associated with mineralization based on previous zircon U-Pb data. Our fluid inclusion study indicates that the ore-forming fluid was oxidized and contained Na, K, Ca, Fe, Cu, Mo, Cl and S. The magmatic-hydrothermal transition occurred at ~425 °C under lithostatic pressure, while potassic, propylitic and phyllic alteration occurred at hydrostatic pressure with temperature progressively decreasing from 425 to 280 °C. The fluid inclusion data presented here suggests that there has been ~2.3 km of erosion at Qulong after its formation,
and this erosion may be related to regional uplift of the Lhasa Terrane.

Rhenium-Osmium geochronology and oil-source correlation of Duvernay Petroleum System, Western Canada Sedimentary Basin: Implications on the application of Re-Os geochronometer on petroleum system

Liu, J. & Selby, D.
PhD Student 25

The rhenium-osmium (Re-Os) geochronometer has been successfully applied to many petroleum systems worldwide to propose directly date the timing of petroleum generation, and also as an oil-source correlation tool. However, debate still remains on what the Re-Os chronometer in petroleum is recording, for example the timing of oil generation or migration. In this study, the direct dating and correlation of a petroleum system by the Re-Os are scrutinized with a simple petroleum system, the Duvernay petroleum system of Western Canada Sedimentary Basin. Despite the low Re and Os abundances in the petroleum, a Re-Os age of 66 ± 31 Ma (n = 14, MSWD = 6.7, initial $^{187}Os/^{188}Os$ = 0.77 ± 0.20) defined by the asphaltene fractions of the oil. This age is in agreement with the geological models proposing oil generation occurred during the Laramide Orogeny. Further we show that the $^{187}Os/^{188}Os$ compositions of source rock, the Late Devonian Duvernay Formation, at the time of oil generation, are distinct from those of other potential source rocks in the basin. Moreover, the the 187Os/188Os compositions of Duvernay Formation at the time of oil generation are similar to those of the $^{187}Os/^{188}Os$ compositions of the oil at the time of formation, and hence supports the previous hypothesis that Os isotopes provide a powerful tool to correlate an oil to its source Formation. In conclusion, this study shows that the Re-Os geochronometer of petroleum can provide the timing of oil generation and be utilized as a correlation tool.

Variations of $^{187}Os/^{188}Os$ through late Permian and implication for paleoenvironment, Lianyuan basin, South China

Liu, Z. & Selby, D.
PhD Student 26

The records of variations, over geologic time, of the isotopic compositions of sea water contribute in special ways to the understanding of the Earth's history. In this study, we present a high-resolution initial osmium isotope stratigraphy of the upper Permian strata. These data are predominantly controlled by the mass balance of two end-member Os isotope components: weathered continental crust (~1.4) and mantle inputs (0.13) attributed to enhanced submarine volcanism. This, coupled with the short residence time of Os in seawater, makes $^{187}Os/^{188}Os$ composition an excellent monitor of palaeoceanographic changes in the geological.

Re abundances range from 0.15ppb to 7ppb, with slightly increase upward and Os abundances range from 20ppt to 150ppt, with a large increase upward. Based on the GSSP time scale, initial Os ratio is calculated at 254Ma and the data show a steady decrease in the lowest part. We lack the data to know how the Osi change from radiogenic Osi value (~1.1) to unradiogenic value (~0.4). This unradiogenic shift may be related to the volcano activity but we still need detailed analysis to figure out the trigger. According to the study of Liao et al (2016), this Osi change is also possibly related to the change in the organic matter type from terrigenous to marine as a result of transgression.

The Delamination and Underplating of the Subducting Crust, and Slow Subduction

Maunder, B., van Hunen, J., Magni, V. & Bouilhol, P.
PhD Student 27

Subducted, compositionally buoyant, crustal materials may form instabilities at the slab-mantle wedge interface which have the potential to feed crustal plumes that rise through the mantle wedge. The end result of this would be underplating of slab crustal material, below the over-riding plate, beneath arcs. This behaviour has been invoked to explain many features of arc magmatism, from variable sedimentary geochemical signatures to its discrete nature in space and time. It has also been proposed as a key mechanism that has led to the formation of Earth's continental crust, at least in part, over time.

We set up a 2D, dynamic, numerical model of subduction with a compositionally layered subducting crust in order to investigate this process of crustal delamination and underplating (often termed "relamination"). Upon undertaking a parameter sensitivity study of this model we recognise that subduction convergence rate has a particularly strong control on this behaviour with slow subduction zones favouring the formation of crustal instabilities. Therefore, we further quantify the effect of subduction velocity on the rate of crustal material flux into the mantle wedge and the composition of this delaminated material. A detailed literature study of observed arc magmatism throughout the Cenozoic, exhibits a correlation between convergence rate and certain geochemical signatures, often suggested to be linked with the melting of crustal materials in subduction zones. Here, we propose and illustrate that this correlation requires, the operation of crustal "relamination" in slow subduction zones.

Bayesian uncertainty analysis for advanced seismic imaging - Application to the Mentelle Basin, Australia

Michelioudakis, D.G., Hobbs, R.W. & Caiado, C.C.S.
PhD Student 28

Quantifying the depths of target horizons from seismic reflection data is among the most important aspects of exploration geophysics. Here, we apply Bayesian methods, to estimate

the uncertainties of the depths of drilling targets for the International Ocean Discovery Program (IODP), leg 369 (SW Australia).

The Mentelle Basin is a deep water sedimentary basin, located between the Naturaliste Plateau and the southern part of the Western Australian Shelf. It hosts a continuous shale sequence that it is over a kilometer thick, the study of which, is crucial for the correlation between the paleoclimate conditions and the tectonic history of the region.

Using 2D multichannel seismic reflection profiles around the drill site, we generate detailed isotropic velocity models for the well location in order to construct initially the optimum Pre – stack time (PSTM) and eventually the Pre - stack depth migrated (PSDM) subsurface images.

The best velocity model created from the initial processing serves as the prior information to the Bayesian model. The goal is to build a multi-layered model of n layers and estimate the zero offset two way time, t_0, and the interval velocities, V_i , for isotropic ($V_{x_i} = V_{z_i}$) case, in terms of a multivariate posterior distribution.

The novelty of our approach compared to the traditional semblance spectrum velocity analysis is the calculation of uncertainty of the output model. Therefore, we can compare the depths from PreSDM following a standard processing sequence, with those extracted from the Bayesian algorithm and the true values from the DSDP - 258. The depths extracted using our algorithm are comparable with those retrieved from the core DSDP-258, showing that the Bayesian model is able to estimate the uncertainty to the drilling targets.

The architecture and frictional properties of faults in shale

Murray, R., De Paula, N., Imber, J. & Holdsworth, R.E.

PhD Student 29

The geometry of brittle fault zones and associated fracture patterns in shale rocks, as well as their frictional properties at reservoir conditions, are still poorly understood. Nevertheless, these factors may control the very low recovery factors (25% for gas and 5% for oil) obtained during fracking operations.

Extensional brittle fault zones (displacement ≤ 3 m) cut exhumed oil mature black shales in the Cleveland Basin (UK). Fault cores up to 50 cm wide accommodated most of the displacement, and are defined by a stair-step geometry. Cores typically show a poorly developed damage zone, and a sharp contact with the protolith rocks. Their internal architecture is characterised by four distinct fault rock domains: foliated gouges; breccias; hydraulic breccias; and a slip zone up to 20 mm thick, composed of a fine-grained black gouge.

Velocity-step and slide-hold-slide experiments at sub-seismic slip rates (microns/s) were performed in a rotary shear apparatus under dry, water and brine-saturated conditions, for displacements up to 46cm. Both the protolith shale and the slip zone gouge display shear localization, velocity strengthening behaviour and negative healing rates. Experiments at seismic slip rates (1.3 m/s), performed on the same materials under dry conditions, show that after initial friction values of 0.5-0.55, friction decreases to steady-state values of 0.1-0.15 within 10 mm of slip. Contrastingly, water/brine saturated gouge mixtures, exhibit instantaneous low steady-state sliding friction of 0.1.

Field observations show that brittle fracturing and cataclastic flow are the dominant deformation mechanisms in the fault core, where slip localization may lead to the development of a thin slip zone composed of fine-grained gouges. The velocity-strengthening behaviour and negative healing rates observed during laboratory experiments, suggest that slow, stable sliding faulting should take place within the protolith rocks and slip zone gouges. This behaviour will cause slow fault/fracture propagation, affecting the rate at which new fracture areas are created. During slipping events, fluid circulation may be

very effective along the fault zone at dilational jogs – where oil and gas production should be facilitated by the creation of large fracture areas – and rather restricted in the adjacent areas of the protolith, due to the lack of a well-developed damage zone and the low permeability of the matrix and slip zone gouge. Finally, experiments performed at seismic slip rates show that seismic ruptures may still be able to propagate in a very efficient way within the slip zone of fluid-saturated shale faults, due to the attainment of instantaneous weakening.

Testing the late veneer hypothesis with Os stable isotopes

Nanne, J.A.M., Millet, M.-A., Burton, K.W., Dale, C.W., Nowell, G.M., Harvey, J. & Williams, H.M.

PhD Student 30

During planetary differentiation, osmium is quantitatively extracted into metallic cores, leaving planetary mantles strongly depleted in Os. The abundance of Os in Earth's mantle is, however, much higher than predicted from metal-silicate equilibration experiments. One common explanation for this overabundance is the late accretion of Os-rich meteoritic materials ('late veneer') after core formation had ceased. In order to test this hypothesis, we have obtained the Os stable isotope composition of chondrites (building blocks of Earth), iron meteorites (representing planetary cores) and compared them to that of the Earth's mantle.

Chondrites show homogeneous stable isotope composition (δ190Os of +0.12±0.04‰; 2sd), suggesting that the solar nebula was homogeneous for Os stable isotopes. Terrestrial samples including geostandards and mantle xenoliths from Kilbourne Hole (USA), show a range in δ190Os from 0.03 to 0.22‰ with an average that is similar to that of chondrites (+0.15±0.03‰; 2sd). That terrestrial mantle samples display chondritic stable Os isotope compositions, suggests that if any stable isotope fractionation occurred as a result of metal-silicate segregation during core formation, it was overprinted by a subsequent late veneer. Finally, iron meteorites display a substantial range relative to chondrites, varying from +0.05 to +0.49‰. The isotopically distinct signature observed in iron meteorites relative to chondrites suggests that core formation processes have the potential to substantially fractionate stable Os isotopes. The variation observed is most likely a result of fractional crystallisation processes of metal alloys. Future research will focus on Archean rocks to investigate mixing of the late accreted material into Earth's mantle.

Deep Palaeozoic Karst: Geothermal Potential In Britain

Narayan, N., Gluyas, J., Adams C. & Imber, J.

Funded by UKOGL

PhD Student 31

Since 2004 the UK has been a net energy importer, with an alarming 46% of energy imported in 2014. In 2013, 48% of the total energy consumed was attributed to heating, with 71% of the heat sourced from gas supplies (50% of which were imported). The rising issue of energy security and the growing demand for heat could be challenged by an advancing geothermal sector. Geothermal prospects already explored across Britain include the fracture-hosted brines in the Weardale granite (46.2°C brines; ~1km depth) and the Southampton borehole sedimentary aquifer (76°C waters; 1.8km depth). However, the 1970s to mid-1980s nationwide geothermal resource assessment, undertaken by the BGS, suggested a lack of economic viability in pre-Permo-Triassic strata thus resulting in untimely omission of potential resources such as Lower Carboniferous Limestone karst. Lower Carboniferous Limestone beds exhibit magnificent karst features, observable in the Mendips, Derbyshire and the Yorkshire Dales, and thermal springs, such as the 47°C spring waters at Bath Spa, suggest that these carbonates host thermal waters at depth. Evidently, these

fractured and karstified limestones therefore potentially accommodate sufficient porosity and permeability to transmit warm waters at significant depths. For example, Milton Green-1 (Cheshire Basin), has recorded flows of 1916 BWPD at depths approaching 1.5km due to the vuggy nature of the Dinantian and Ridgeway Borehole (Sheffield) recorded 48.9°C waters at the top of the Carboniferous Limestone at 883m depth, with flows of 100,000 gallons per day. This project aims to explore the Carboniferous Limestone karst resources available nationwide through, 2D seismic data analysis of unconformable karst surfaces, the analysis of deep cores, a compilation of existing porosity and permeability data analyses from literature and well data and geothermometry investigations through utilisation of spring water data. A final output will be a compiled resource inventory, characterising the limestone karst and the size of the available resource.

Landscape maturity and fold growth timing in the Kirkuk Embayment of the Zagros, northern Iraq

Obaid, A.K. & Allen, M.B.
PhD Student 32

The Kirkuk Embayment is located in the southwestern part of the Zagros fold–and-thrust belt of Iraq. Like fold-and-thrust belts worldwide, the Zagros is conventionally understood to have grown sequentially from the hinterland towards the foreland, i.e. from northeast to southwest, either in a series of tectonic pulses or a more continuous progression. Here we use landscape maturity analysis to understand the development of anticlines in the Kirkuk Embayment, and hence the tectonic evolution of the region. DEM-based geomorphic indices Hypsometric Integral (HI), Surface Roughness (SR) and their mathematical combination Surface Index (SI) have been applied to quantify landscape maturity. Topographic position Index (TPI) has also been used to investigate the effects of deformation on the landscape. The results are relevant to the growth sequence of anticlines within the Kirkuk Embayment, which is a major hydrocarbon province. The growth sequence is not consistent with classical 'piggy back' thrusting in a simple critically tapered wedge; the maturity indices are highest for the QaraChauq anticline in the center of the Embayment, then the Makhool/Himreen anticline to the south and, lastly, the Kirkuk anticline to the north. This pattern fits the exhumation record, which is loosely constrained by the level of exposed stratigraphy within the fold cores: QaraChauq exposes the oldest strata of the three main folds considered. The favored hypotheses for the order of fold growth are either i) the folds have grown at different time and out of sequence (QaraChauq first, then Makhool/Himreen, and Kirkuk last), or, ii) the growth occurred with different rate of exhumation but at broadly the same time. There are few constraints from available data on syn-tectonic sedimentation patterns, but it may be that fold growth across much of the Embayment began within a limited timeframe in the late Miocene – Pliocene (?), during the deposition of the Mukdadiyah (Lower Bakhtiari) Formation. TPI analysis helps identify two new anticlines in a region where they have not been described before. TPI could be used in the discovery of anticlines of importance for oil exploration in the region.

The Significance of Fluid Pressure on Sandstone Diagenesis

Oye, O., Aplin, A., Jones, S. & Gluyas, J.
PhD Student 33

It is well known that the development of shallow overpressure in sandstone reduces vertical effective stress (VES), preserving porosity and economic reservoir quality. However, the influence of pore pressure on chemical compaction ("pressure solution") and related quartz cementation in sandstones has been deemphasized in several clastic reservoir studies

that have favoured temperature as the only relevant driver. This study is targeted at understanding the relevance of VES to the rate of quartz cementation by investigating the shallow marine sandstone of the Upper Jurassic Fulmar in the UK Central Graben. Samples have been chosen from sandstones which have been buried to a wide range of pressures and temperatures. First results are from the upper shore-face sands of the High Pressure High Temperature (HPHT) Elgin field (UK Quad 22), in which pore pressures are in excess of 100MPa (overpressures over 50MPa) and temperatures around 190oC at depths greater than 5000mbsf. Porosities are of up to 31%, and evidence from modal analysis of thin section from optical microscopy revealed average primary porosities of around 11%b.v. (range of 2 to 21%). Despite the high temperature, average quartz cement contents are only around 2%b.v, lending credence to the idea that chemical compaction and quartz cementation may be suppressed by low VES.

Madagascar's escape from Africa: New fracture zone trends and geodynamic understanding from gravity data

Phethean, J.J.J.
PhD Student 34

We present a new plate tectonic reconstruction for the drift of Madagascar away from East Africa using the new Sandwell and Smith gravity dataset. Detailed analysis of the free-air gravity anomaly, vertical gravity gradient, and horizontal derivatives of filtered gravity (used to enhance spreading lineaments from heavily sedimented ocean basins) allow us to identify the extinct mid-ocean ridge and associated spreading lineaments in the Western Somali Basin. Identification of the mid-ocean ridge segments provides a means to identify the basin's centre of symmetry, which can be compared directly to ocean magnetic anomaly interpretations for the Western Somali Basin. Interpretations of the basin's symmetry based on the M0 magnetic anomaly are found to be most reliable, and are therefore used in conjunction with the gravity-derived spreading lineaments to produce a temporally constrained plate tectonic reconstruction.

This reconstruction supports a tight fit for Gondwana fragments prior to breakup, and predicts that the continent-ocean transform margin lies along the Rovuma Basin, not along the Davie Fracture Zone (DFZ) as previously thought. This is supported by new seismic evidence for oceanic crust inboard of the DFZ, and changes the direction, position and style of the continental margin offshore Mozambique and Tanzania. The Tanzania Coastal Basins should be considered as an oblique, and likely segmented, rifted continental margin. We also show the DFZ to be a major ocean-ocean fracture zone formed by the coalescence of several smaller fracture zones during a change in plate motions as Madagascar escaped from Africa.

Fault lubrication at seismic slip rates due to viscous flow in nanometric gouges?

Pozzi, G.
PhD Student 35

Recent studies have demonstrated that the friction coefficient of faults drops dramatically from Byerlee's values (0.6-0.8) to very low steady values of 0.1-0.2 when sheared at seismic slip rates (~1m/s). However, very little is understood about the microscale weakening mechanisms that ultimately control earthquake rupture propagation. We performed shear experiments on calcite gouges in a low to high velocity rotary shear apparatus at normal stresses up to 25MPa and slip rates up to 1.4 m/s. The measured friction coefficient drops from peak values of 0.8-0.9 to steady-state values as low as 0.2-0.4 when approaching seismic slip rates (> 0.1m/s). The amount of slip required for the onset of weakening is inversely proportional to the slip velocity and the normal stress. Microstructural analysis on deformed samples shows particle comminution up to nanometric scale (<1μm), even

after small amount of slip, and strain localisation into a thin slip zone (<200μm). Samples that underwent steady-state weakening formed specular shiny slip surfaces paved by low-porosity aggregates of polygonal recrystallized calcite grains (~600-700μm), sandwiching a layer of finer particles. We interpret that a sharp strain gradient is present at the boundaries of this layer (possibly decoupled), with sin-shearing grain growth occurring in the neighbouring low-strain domains. These evidences suggest that extreme localisation promotes grainsize-dependent thermal weakening. Flow stresses predicted by grain boundary sliding flow laws agree with those measured during the experiments at high velocity (>10 cm/s) and normal stress (25MPa).

Coupled thermodynamic and two-phase flow modelling of partially melting crust

Riel, N.[1], Bouilhol, P.[1], van Hunen, J.[1] , Magni, V.[1], Velic, M.[2] & Cornet, J.[1]

[1]Durham University; [2]University of Melbourne

PhD Student 36

How magmas are formed, transferred and interact in the lower crust to form mid-crust plutonic belts remain a fundamental question to understand the chemical and mechanical evolution of continents. To assess this question we developed a 2-D two-phase flow code using finite volume method. Our formulation takes into account: (i) an extended Darcy's law for fluid flow with first order temperature- and fluid-content dependency for the host-rock viscosity and silica-dependent viscosity for the fluid, (ii) the heat equation assuming thermal equilibrium for both solid and liquid and temperature-dependent diffusivity, (iii) thermodynamic modelling of stable phases via a dynamic coupling with Perple_X, and (iv) chemical advection of both the solid and liquid composition. To model chemical interactions with the host rock during magma transport, the melt is assumed to be either in thermodynamic equilibrium or in thermodynamic disequilibrium, or as function of these two endmembers.

We applied our modelling approach to investigate the behaviour and composition of magma during lower crust melting. Our goal is to better understand the formation of felsic crust through melting, segregation and assimilation of lower crustal lithologies, applied to Archaean systems. Our preliminary results show the ascend of silica-rich magmas is slow, occurring on the timescale of millions of years, and is highly controlled by (i) the melting curve of the protolith and (ii) by its chemical degree of interaction with the host rock. The resulting transferred magmas are in good accordance with observed composition forming the grey gneisses of Archean terranes (i.e SiO2-rich > 62%, Mg# = 40-50, Na2O ~6%, MgO = 0.5-1%).

Modelling Seismic Wave Propagation within Extrusive Basalt Sequences

Sanford, O.G.[1], Hobbs, R.W.[1], Johnston, C.[1] , Brown, R.J.[1] & Schofield, N.[2]

[1]Durham University; [2]University of Aberdeen

PhD Student 37

Layers of highly heterogeneous basalt flows within sedimentary successions (e.g. in the Faroe-Shetland Basin) cause complex scattering and attenuation of seismic waves during seismic exploration surveys. Typically, the refracted wave from the basaltic layer is used to build a velocity model by tomography. This velocity model is then used to aid seismic data processing, and may also be used as part of assessing drilling risk of potential wells, as it is believed to constrain the total thickness of the sequence.

In heterogeneous media, scattering preferentially traps the seismic energy in the low velocity regions. This causes a build up of energy that is guided along the low velocity layers. This has implications for the interpretation of the observed first arrival of the seismic wave, which may be a biased towards the low velocity regions, and will lead to an underestimate of the velocity structure, and hence the thickness of the basalt.

Using 2-D acoustic finite difference modelling of

the refracted wave through simple basalt sequences, we consider the relative importance of different properties of the basalt on the seismic energy propagating through the layers. These include the proportion of high to low velocity material and the roughness of the interfaces between the layers. We observe a non-linear relationship between the ratio of high to low velocity layers and the apparent velocity of the first arrival, suggesting that such a sequence may cause a reduction of the apparent velocity by as much as 1.5 km s^{-1}.

Controls on the location of arc volcanoes: An Andean study

Scott, E.M., Allen, M.B., McCaffrey, K.J.W., Macpherson, C.G., Davidson, J.P. & Saville, C.
PhD Student 38

Across the entire Altiplano-Puna Plateau (APP), South America, Quaternary arc volcanoes are found to be either at or above the 3500 m elevation contour, which also defines the cut off for seismogenic thrusting. Depth corrected data of earthquake hypocentres are used to generate new models of depth to the subducting Nazca slab beneath the APP. This new slab model shows a general correlation between the 100 km depth to the slab, the western edge of the APP and the frontal volcanic arc. The exception to this correlation is the region of the Salar de Atacama basin (SdAb, 23-24o S); a major break in topography on the west side of the APP. Here, the volcanic arc steps approximately 80 km to the east in comparison to the general trend of the arc. Arc volcanoes follow the eastern edge of the basin and remain above 3500 m. The volcanoes bordering the SdAb have a depth to slab approximately 30 km deeper than those in the adjacent arc segment 200 km to the north of the basin. Across this distance there is no significant difference in subduction parameters so the factors affecting the melt source are constant. It is likely, therefore, that melt forms at the same depth in both locations; however, in the case of the Salar de Atacama region, magma is diverted to the east due to preferential emplacement under higher elevations of the plateau.

Importance of vertical effective stress for reservoir quality; examples from the Skagerrak Formation, Central Graben, North Sea

Stricker, S.[1], Jones, S.J.[1] & Grant, N.T.[2]
[1]Durham University; [2]ConocoPhillips UK Ltd.
PhD Student 39

The complex fluvial sandstones of the Triassic Skagerrak Formation are the host reservoir for a number of high-pressure, high-temperature (HPHT) fields in the Central Graben, North Sea. All the reservoir sandstones in this study comprise of fine to medium-grained sub-arkosic to arkosic sandstones that have experienced broadly similar burial and diagenetic histories to their present-day maximum burial depth. Despite similar diagenetic histories the fluvial reservoirs show major variations in reservoir quality and preserved porosity. Reservoir quality varies from excellent with anomalously high porosities of up to 35% at burial depth of >3500 m to poor with porosities <10% at burial depth of 4300 m. This study has combined detailed petrographic analyses, core analysis and pressure history modeling to assess the impact of differing vertical effective stresses (VES) and high pore fluid pressures (> 80 MPa) on reservoir quality. It has been recognized that fluvial channel sandstones of the Skagerrak Formation in the UK sector have experienced significantly less mechanical compaction than their equivalents in the Norwegian sector. This difference in mechanical compaction has had a significant impact upon reservoir quality, even though the presence of chlorite grain coatings inhibited macroquartz cement overgrowths across all Skagerrak Formation reservoirs. It is the cumulative effect of varying amounts of overpressure and its effect on the VES history that is key to determining the reservoir quality of these channelised sandstone units. The results are

consistent with a model where vertical effective stress affects both the compaction state and subsequent quartz cementation of the reservoirs.

Environmental and anthropogenic factors affecting the respiratory toxicity of volcanic ash in vitro

Tomašek, I., Horwell, C.J., Damby, D.E., Ayris, P.M., Barošova, H., Geers, C., Petri-Fink, A., Rothen-Rutishauser, B. & Clift, M.J.D.

PhD Student 40

Human exposure to inhalable volcanic ash particles following an eruption is a health concern, as respirable-sized particles can potentially contribute towards adverse respiratory health effects. Although there is substantial information on the mineralogical properties of volcanic ash that may influence its biological reactivity, knowledge as to how external factors, such as air pollution, contribute to the potential reactivity is limited.

To gain a first understanding of the biological impact of the respirable fraction of volcanic ash when exposed simultaneously with diesel exhaust particles (DEP) in vitro, we used a sophisticated 3D triple cell co-culture model of the human alveolar epithelial tissue barrier. The multi-cellular system was exposed to DEP and then exposed to either a single or repeated dose of well-characterised respirable volcanic ash from the Soufrière Hills volcano, Montserrat for a period of 24 hours. Cultures were subsequently assessed for adverse biological endpoints including cytotoxicity, oxidative stress and (pro)-inflammatory responses. Results indicated that the combination of DEP and respirable volcanic ash at sub-lethal concentrations incited a release of (pro-)inflammatory markers that was greater, in some circumstances, than the response for either DEP or volcanic ash, independently.

Further work is planned, to determine if this effect is maintained for ash exposure concurrent with complete vehicle exhaust, as well as with samples exposed to an experimentally-simulated volcanic plume environment. It is envisaged that the findings of this study will provide a better understanding of the potential risk posed by combined exposure to urban pollution and volcanic ash towards human health.

Molecular dynamic simulations of low-salinity enhanced oil recovery

Underwood, T.

PhD Student 41

The aim of this research is to bring clarity to the fundamental mechanisms of clay-oil-brine interfaces that underpin low-salinity enhanced oil recovery (EOR), a technique whereby sea water, partially desalinated, is used to push increasing amounts of crude oil from existing, and future, oil reservoirs, increasing the reservoir lifetime and overall production. The phenomenon of low-salinity EOR is thought to be due to the complex interactions between the organic oil compounds, clay particles and the salt ions within the reservoir.

Using large-scale molecular dynamics (MD) simulations to model the interactions of several different clays (chiefly montmorillonite and kaolinite) interacting with various model oil compounds, we have been able to analyze the phenomena of low-salinity EOR at the molecular level.

Our work presents an increasingly high-resolution picture of low-salinity EOR, whereby it is observed that the effects of double layer expansion cannot explain the phenomenon of low-salinity enhanced oil recovery. Rather, the results show that it is the pH level surrounding the clay in conjunction with the presence of divalent cations that is the determining factor driving the titular effect [1, 2]. The research highlights several key conditions required for a low-salinity EOR flood to function, and successfully presents how nanoscale simulations can help describe macroscopic phenomena.

[1] Underwood, Erastova, Cubillas & Greenwell, (2015) *J Phys.Chem. C* **119.13**: 7282-7294.
[2] Underwood, Erastova & Greenwell (2016) *J. Phys. Chem. C* **(Accepted)**

Mechanisms controlling the modes of slab sinking through the transition zone

Agrusta, R.
Postdoctoral Research Assistant 42

It is generally accepted that subducting slabs can either sink straight into the lower mantle, or lie down in the mantle transition zone. Several studies have suggested that the key parameters to control whether slabs stagnate or penetrate may be one or more of: trench motions, slab strength, slab age, subduction of buoyant features, overriding plate forcing, and/or density and viscosity changes associated with the transition to the post-spinel phase. In this study, using 2D self-consistent thermo-mechanical subduction models, we investigate which parameters are most efficient in allowing slabs to penetrate or to stagnate above the lower mantle, and which allow the mode of slab-transition-zone interaction to change in time from penetrating to stagnant and also vice versa. Over a wide range of plausible Clapeyron slopes and viscosity jumps at the base of the transition zone, young slabs penetrate while older slabs drive more trench motion and stagnate. We found several mechanisms able to induce a change from stagnation to penetration: an instantaneous change in the forcing of the upper plate from free to fixed leads to a rapid change in mode, while a sudden change in the Clapeyron slope (as might be possible due to dehydration of the slab) has a relative slow effect. Suddenly changing the age at the trench from old to young does not show any change. Whereas the reverse change in upper plate forcing or subducting-plate age is able to make penetrating slabs stagnate.

Natural and anthropogenic forcing of North Atlantic tropical cyclone track position since 1550 A.D.

Baldini, L.M., Baldini, J.U.L., McElwaine, J.N., Ridley, H.E. & Macpherson, C.G.
Postdoctoral Research Assistant 43

Over the last 30 years, North Atlantic tropical cyclones (TC) have increased in frequency, intensity, and duration in response to rising North Atlantic sea surface temperatures (SST). Here we present a 450-year record of western Caribbean TC activity reconstructed using subannually-resolved carbon and oxygen isotope ratios in a stalagmite from Yok Balum Cave, southern Belize. Western Caribbean TC activity peaked at 1650 A.D. coincident with maximum Little Ice Age cooling and decreased gradually to 1983 A.D. (the end of the record). Comparison with existing basin-wide reconstructions reveals that the dominant TC tracks corridor migrated from the western Caribbean toward the North American east coast through time. A close link with Atlantic Multidecadal Oscillation (AMO) exists throughout the record but with a clear polarity shift in the TC-AMO relationship at 1870 A.D., coincident with industrialisation. We suggest that the cause of this reversal is Greenhouse gas and aerosol emission induced changes in the relationship between the Intertropical Convergence Zone and the Bermuda High between the modern warm period and the Pre-Industrial Era. The likely impact of continued anthropogenic forcing of TC track on population centres of the western North Atlantic and Caribbean will be addressed.

Assessing the fugitive emission of CH_4 via migration along fault zones – comparing shale basins to non-shale basins

Boothroyd, I.M., Almond, S., Worrall, F. & Davies, R.J.

Postdoctoral Research Assistant 44

Fault zones and fracture networks have the potential to act as conduits for fluid flow and gas migration to groundwater aquifers and the surface, where fugitive emissions of greenhouse gases to the atmosphere can take place. It is important to understand the extent to which fault zones enhance fluid flow from hydrocarbon basins to the surface when considering the possible impacts of hydraulic fracturing in shale gas basins on the environment.

This study compares methane (CH_4) concentrations across five fault systems in the UK using real-time mobile monitoring techniques. A Picarro Surveyor cavity-ring-down spectrometer was used to measure concentrations of CH_4 and $\delta^{13}C\text{-}CH_4$ to allow identification of thermogenic and biogenic CH_4 sources. The study was conducted along faulted and non-faulted control routes in two shale gas basins, two coal basins and a non-hydrocarbon control basin.

Analysis of variance indicated that fault routes had higher concentrations of CH_4 than non-faulted control routes, while differences between basins explained the most variation in CH_4 concentration. Binary logistic regression highlighted the impact of elevated concentrations of CH_4 from landfill sites and agricultural areas, but was not sensitive enough to detect differences between fault and control routes. The average flux of faults over and above that expected from the background was 0.27 ± 0.14 $kgCH_4$/km of fault/day or 0.1 ± 0.05 tonnes CH_4/km of fault/yr), however, this flux is concentrated onto certain locations on certain faults and it is not known what length of faults across the UK we should consider.

Cayman Trough, Caribbean Sea: crustal accretion and transform margin evolution at ultra-slow spreading rates

Castiello, G., Peirce, C., Pitcairn, B., Bird, A. & Clegg, A.

Postdoctoral Research Assistant 45

About 57% of the Earth's surface is covered by oceanic crust and new ocean floor is continuously created along the ~65,000 km long mid-ocean ridge (MOR) system. 25% of the MOR spread at an ultra-slow spreading rate of <20 mm/yr. At ultra-slow spreading rates the melt supply to the ridge is thought to dramatically decrease and crustal thicknesses reduce to <6 km. We know little about the processes generating oceanic crust at slow spreading rates. Formation of crust from a magma chamber would suggest the creation of a well stratified crust, with an extrusive upper crust, a lower gabbroic crust and a well-defined crust-mantle boundary and hence a seismic Moho. In contrast, decompressional melting without formation of a magma chamber would support a crustal structure where seismic velocities change gradually from values typical of crustal to mantle rocks. The Cayman Trough is an example of ultra-slow spreading centre. Here we describe its characteristics and focus mainly on the study of the transform margin evolution at the Swan Island Transform Zone (SITZ). The SITZ is a segment of the plate boundary between the North American and Caribbean plates and bounds the southwestern side of the trough. Our objectives are to determine:

1) if lateral motion along the SITZ occurs along a single fault or within a fault zone and how the motion between oceanic and continental lithosphere is accommodated,

2) the thickness of the continental crust and the lateral coupling between that and the oceanic crust.

Volatiles in arc plumbing systems: Insights from cumulate hosted melt inclusions, Lesser Antilles

Cooper, G.F., Davidson, J.P. & Blundy, J.D.
Postdoctoral Research Assistant 46

The Lesser Antilles Arc has an exceptional abundance and variety of erupted plutonic xenoliths, which represent crustal storage regions. The xenoliths provide a window into the arc crust and a deeper evolutionary history than is possible from lavas alone, which commonly only represent the end products of magmatic processes.

Volatiles, in particular H_2O, have a fundamental control on the generation and differentiation of magmas at subduction zones. We aim to place constraints on the conditions of cumulate crystallisation, the input of volatiles from the mantle wedge and the distribution of volatiles both through the crust and along the length of the arc.

Melt inclusions (MI's), trapped in crystal phases and interstitial glass within plutonic xenoliths from St. Eustatius, Dominica, Grenada and St. Vincent, were analysed for major elements by EPMA, and H_2O, CO_2 and selected trace elements by Ion Microprobe.

Analysed melts display significant major and trace element variations. The majority of MI's and interstitial glass fall into two groups with a compositional gap at 56-66 wt.% SiO_2 and 1.2-2.5 wt.% MgO. Interstitial glass is commonly less evolved than MI's, suggesting mobilisation of the cumulate/mush pile by ascending melts.
Water concentrations of MI's vary from <0.5 to 9 wt.% H_2O. Some low values of H_2O are likely the result of reequilibration and fluid loss. CO_2 concentrations are generally low (<200 ppm), but a number of inclusions have higher values (up to 1000 ppm). Cl concentrations span a large range (0.1-0.9 wt.%), with the highest values in melts from Grenada, suggesting the involvement of saline fluids.

Dehydration study of Layered Double Hydroxides intercalated with Amino Acids: insights into the Origin of Life

Erastova, V.[1], Degiacomi, M.T.[1] & Greenwell, H.C.[2]
[1]Durham University; [2]University of Oxford
Postdoctoral Research Assistant 47

The role of mineral surfaces in concentrating and facilitating the polymerisation of simple protobiomolecules during the Hadean and Archean has been the subject of much research, in order to constrain the conditions that may have led to the Origin of Life. In this work we examine the behaviour of layered double hydroxide minerals intercalated with six amino acids, upon wetting-drying cycles of the early Earth environment. We use molecular dynamics to highlight the trends and the differences in behaviour of the range of amino acids and their adsorption mechanisms onto the surfaces. We also show how structural rearrangements occur through the dehydration and we assess the potential for further formation of peptide bonds.

The carbon functional group budget of a peatland

Moody, C.S.[1], Worrall, F.[1], Clay, G.D.[2] & Apperley, D.C.[1]
[1]Durham University; [2]University of Manchester
Postdoctoral Research Assistant 48

Organic matter samples were taken from each organic matter reservoir and fluvial flux found in a peatland and analysed by elemental analysis for carbon, hydrogen, nitrogen and oxygen content, and by 13C solid state nuclear magnetic resonance (NMR) for functional group composition. The samples analysed were: aboveground, belowground, heather, mosses and sedges, litter layer, four different depths from a peat core, and monthly samples of fluvial particulate and dissolved organic matter. All organic matter samples were taken from a 100% peat catchment

within Moor House National Nature Reserve in the North Pennines, UK.

The proportion of carbon atoms from each of the eight carbon functional groups (C-alkyl, N-alkyl/methoxyl C, O-alkyl, O2-alkyl/acetal C, aromatic/unsaturated C, phenolic C, aldehyde/ketone C and amide/carboxyl C) from each type of organic matter were combined with an existing carbon budget from the same site, to give a functional group carbon budget. The budget results show that the ecosystem is accumulating N-alkyl/methoxyl C, O-alkyl, O2-alkyl/acetal C and phenolic C groups, but losing C-alkyl, aromatic/unsaturated C, amide/carboxyl C and aldehyde/ketone C. Comparing the functional group compositions between the sampled organic matter pools shows that DOM arises from two distinct sources; from the peat itself and from a vegetation source.

The Origin and Evolution of Oceanic Core Complexes at 13°N on the Mid-Atlantic Ridge

Simao, N.[1], Peirce, C.[1], Searle, R.[1], Falder, M.[2], Reston, T.[2] & MacLeod, C.[3]

[1]Durham University; [2]University of Birmingham; [3]Cardiff University

Postdoctoral Research Assistant 49

Our understanding of the processes of sea-floor spreading at slow-spreading mid-ocean ridges is undergoing a paradigm shift. It is becoming increasingly clear that much of the slowly spread sea-floor has not been built solely by the symmetric accretion of the products of partial melting to the trailing edges of the separating plates as traditional models dictate, but that tectonic stretching on large-offset normal faults, weakened by the penetration of water and production of weak phyllosilicates, also plays a fundamental role, unroofing plutonic and partially serpentinised mantle foot-walls to form oceanic core complexes (OCCs). The detachment processes in itself and the creation of oceanic core complexes is still poorly understood. For example, it is not clear, what their 3D geometry is, how they are linked with the supply and emplacement of magma and, crucially, how far detachments continue laterally in the sub-surface and/or if they link at depth. Our understanding of the 3D geometry and mechanics of detachment faults is limited by a paucity of observations from actively forming OCCs, and by a reliance on sea-floor imagery alone at these locations to make interpretations. Fortunately, an extensive region of OCCs exists at 13°N on the MAR, including two that are recognized as being active and traceable to the spreading axis. Only by determining the internal structure of actively evolving OCCs and how they are connected can we hope to test different models in this way discerning between conflicting hypotheses and have their uncertainties resolved.

A global review of anthropogenic related seismicity

Wilson, M.P., Foulger, G.R., Gluyas, J.G. & Davies, R.J.

Postdoctoral Research Assistant 50

In recent years the awareness of earthquakes related to human activities has grown both within the scientific and public communities. The industrial operations of hydraulic fracturing (fracking) and deep subsurface waste water disposal have been the primary cause of this interest, particularly because of the large increase in seismic rate in the central USA. Despite this renewed interest, it has long been known that the human activities of conventional oil and gas operations, geothermal reservoir exploitation, groundwater extraction, subsurface fluid disposal, mining, water reservoir construction and underground nuclear explosions can lead to earthquakes.

Here we present the world's largest database of anthropogenic related earthquakes caused by induvial human projects. This database stands at over 600 cases based on peer-reviewed published literature and various reports and presentations.

As well as recording the sites of anthropogenic earthquakes, this database also contains important data, such as fluid injection volumes, which may help improve our understanding of the factors and mechanisms of anthropogenic earthquakes.

With an ever increasing world population and a growing demand for resources, it is vital that resources can be exploited in a safe and responsible manner. The additional pressure of climate change will likely require the subsurface geostorage of carbon dioxide. Whilst this activity will reduce the effects of climate change, it will increase the risk of earthquakes and it is therefore necessary that we aim to mitigate and reduce this potentially harmful effect.

3D crustal structure beneath the Costa Rica Rift from seismic refraction tomography

Zhang, L.[1], Wilson, D.J.[2], Tong, V.C.H.[1] & Hobbs, R.W.[2]

[1]University College London; [2]Durham University

Postdoctoral Research Assistant 51

The Costa Rica Rift is situated on the eastern arm of the Cocos-Nazca spreading centre, in the Panama Basin. It is a 140 km long ridge segment bounded by the Ecuador fracture zone to the west and the Panama fracture zone to the east. The Costa Rica Rift is spreading at an intermediate rate with slight asymmetry indicated by a half rate of 30 mm yr-1 to the north and 36 mm yr-1 to the south. We deployed 25 ocean-bottom seismographs (OBS) in a 5 X 5 grid covering an area 35 x 35 km2 over the ridge axis. A total of ~62,000 first-arrival refraction events were picked from the OBS records and used to invert for the P-wave velocity structure. By using First-Arrival Seismic Tomography (FAST) modelling, we obtain the 3D velocity-depth model. The results show that at the ridge axis, a ~5 km-wide relatively low-velocity zone (LVZ) extends downwards at the depths greater than 1.0-1.5 km below seafloor. The width of LVZ increases to 10 km at 2.5-3.5 km below seabed. The shallow LVZ indicates either recent accretion of basalt in the upper crust and/or high porosity/crack density. The deeper, wider LVZ may indicate a higher melt fraction in the crust, representative of an axial magma chamber. In spite of the noisy quality of NG data, an anisotropic character can be identified, with the fast direction around 90°, implying that zones of increased melt fraction and vertical fractures/faults are oriented nearly parallel to the ridge axis, which has a mean orientation of 92°.

Using high-resolution monitoring data to identify the effects of cave and surface conditions on cave drip water hydrochemistry

Baldini, J.U.L.[1] & Sherwin, C.M.[2]

[1]Durham University; [2]Imperial College London

Academic Staff 52

Hourly-scale cave air PCO2, temperature, barometric pressure, and drip water electrical conductivity and discharge rates were used to demonstrate the effects of prior calcite precipitation (PCP) on drip water chemistry within Crag Cave, Ireland. Lower cave air PCO2 caused more CO2 degassing from drip water and subsequently more PCP, and higher cave air PCO2 reduced PCP, although these effects were minor compared with dilution effects caused by variability in recharge. Calcite growth over the interval of the study was quantified by using an Iceland Spar calcite rhombohedron as a substrate; the total observed calcite growth compared very favourably to values calculated using theoretical calcite growth equations. To our knowledge this is the first study that compares actual and theoretical calcite growth rates calculated using all growth determining variables at a high temporal resolution, and it suggests that equations used to calculate calcite growth rates are valid. The study also demonstrates that PCP is an active process in caves, and is potentially important in modulating drip water chemistry, stalagmite growth rates, and consequently geochemical proxy records contained within stalagmites.

A partial late veneer for the source of 3.8 Ga Isua rocks: Evidence from highly siderophile elements and 182W

Dale, C.W.[1], Kruijer, T.S.[2] & Burton, K.W.[1]

[1]Durham University; [2]University of Münster

Academic Staff 53

Late accretion partially replenished highly siderophile elements (HSE) in planetary mantles after they were strongly sequestered into metallic planetary cores [1]. Ancient isolated domains in Earth's mantle – such as the source of 3.8 Ga Isua basalts – might represent mantle isolated from late accreted material, as inferred from their small 182W excesses compared to Earth's present-day mantle [2]. However, such 182W excesses may instead represent signatures of early mantle differentiation. To assess the origin of 182W anomalies and the 182W composition of the pre-late veneer mantle, we determined HSE abundances and 182W compositions of a suite of mafic-ultramafic rocks from Isua, Greenland.

Our data show that the Isua source mantle had HSE abundances at ~60% of the present-day mantle, with a 13±4 ppm 182W excess. Using a range of possible late veneer compositions, we calculate that the Isua mantle source, containing 60% late veneer, would have a 182W value of 9±4 ppm, in excellent agreement with the measured value for Isua. The combined HSE-W data, therefore, are consistent with only partial late accretion to the Isua mantle source, and with the interpretation that the 27±4 ppm 182W excess of the Moon represents the 182W composition of the pre-late veneer Earth's mantle [4]. This finding supports the idea of disproportional late accretion to the Earth and Moon. In this case, the Isua source represents ambient mantle into which only a part of Earth's full late veneer was mixed, rather than an isotopically distinct mantle domain which survived the giant Moon-forming impact.

[1] Dale et al. (2012) Science 336, 72. [2] Willbold et al. (2011) Nature 477, 195. [3] Touboul et al. (2012) Science 335, 1065-1069. [4] Kruijer et al. (2015) Nature 7548, 534

Taking geology to the IMAX: Real-time 4D tomography for volcanology and beyond

Dobson, K. *et al.*

Academic Staff 54

Geology is inherently dynamic across a wide range of temporal and spatial scales. Whether we work using field, analytical or experimental approaches, most of what we do as geoscientists is "snap shot" sampling: capturing a 2D, or perhaps 3D representation of a spatially and temporally variable problem. True scaling of rates, processes and behaviours from laboratory and hand specimen to the 4D geosphere is still poorly understood, and numerical methods often lack multi-scale validation.

Using micro computed tomography (XCT) we can now visualise the internal structures and spatial associations inside geological samples non-destructively. Furthermore, with the development of true 4D (3D + time) imaging at up to 20 x 3D images per second at micron scale resolution, we are now able to perform in situ observations in real time. New experimental systems are constantly being developed to allow in situ observation of compression, torsion, fracture, multi-phase flow, chemical reactions at temperature (-40 to 1600C) and under pressure.

I present two key examples showing state-of-the-art of in situ 4D imaging, specifically aimed at showcasing capabilities for geoscience applications. The first example comes from volcanology and shows how when working at magmatic temperatures we can image the relative motions of every bubble and crystal in a sample as we deform it: thereby gaining new insight into magma rheology, the interaction between the chemical and physical evolution of the magma, and to develop better understanding of eruption trigger mechanisms. The second example comes from the first real-time imaging of multi-phase reactive flow in porous media, specifically looking at tracing 4D distribution of phases during water, oil and saline solution multi-phase transport in unsaturated sandstones.

Multi-scale Study of the Elastic Response of Organic-rich Shales

Goodarzi, M.[1], Rouainia, M.[1], Cubillas, P.[2] & Aplin, A.[2]

[1]Newcastle University; [2]Durham University

Academic Staff 55

In this study, PeakForce QNM® and nanoindentation were combined to determine the micromechanical properties of shales as a function of mineralogy and organic matter content. Bulk mineralogy and pore systems were characterized using XRD and mercury porosimetry. Thin sections were cut both parallel and perpendicular to bedding, and smooth surfaces prepared by Argon ion milling. Elastic responses were then measured at two different scales. PeakForce QNM® was used to map the elastic response of shales at the scale of few nanometres. The mapped surface was analysed using SEM-EDX in order to relate the mechanical properties to individual shale constituents. Results show that the elastic response of stiff grains (quartz, calcite, pyrite) are isotropic. In contrast, an anisotropic response was observed on the less stiff clay matrix at the scale of few nanometres, comparable to that seen at the core scale. Organic matter was the least stiff constituent.

Nanoindentation was used to measure the elastic response of samples at a scale which combines the individual responses of different minerals and organic matter. PeakForce QNM results for individual phases were then integrated with the nanoindentation results using a homogenisation procedure which assumes that shale is a composite formed by a porous clay matrix in which solid mineral grains/inclusions are randomly distributed. Comparisons between (a) the predictions of the homogenization methods on macroscopic elastic response and (b) the obtained Young's modulus from indentation are good, showing that macroscopic mechanical properties can be understood from the micromechanical data of individual grains and grain composites.

Two-Stage Multi-Particle Sintering of Kimberlitic Volcanic Ash

Haddock, D.[1], Brown, R.J.[1], Jones, T.J.[1], Gernon, T.M.D.[2] & Manya, S.[3]

[1]Durham University; [2]University of Southampton; [3]University of Dar es Salaam

Academic Staff 56

Kimberlite magmas provide important insights into mantle chemistry and physics and are the main carrier of diamonds to the Earth's surface. However, their eruption dynamics remain perplexing primarily due to their unusual rheological properties. Here we present data on unique kimberlite pyroclasts that preserve unequivocal evidence for two-stage multi-particle sintering achieved through viscous flow and melt diffusion at temperatures above the glass transition. The pyroclasts are fragile agglomerates constructed through the sintering of smaller particles (<10–50 μm) onto larger particles (>100–3000 μm), followed by the sintering together of large particles at point contacts on deposition in the conduit. This weakly sintered rock was subsequently fragmented by later explosions, entrained into weak ash plumes, and deposited around the crater of a small Holocene kimberlite volcano in Tanzania. The agglomerates show similarities to less well-preserved rocks in kimberlite pipes worldwide and provide indisputable evidence for the deposition of hot, compound particles during the eruption of kimberlite magmas.

...and the OSCAR goes to...

Hobbs, R.W.[1], Maqueda, M.A.M.[2] , Peirce, C.[1], Tong, V.C.H.[3] & the cast of OSCAR

[1]Durham University; [2]Newcastle University; [3]University College London

Academic Staff 57

After a long and sometimes explosive relationship, Ocean and Crust have decided to divorce. Things eventually came to a rift and they decide to no longer share the same seabed. Crust, looking for a

more solid relationship, has gone off with Mantle who under the right conditions would melt in his arms and between them have produced an illegitimate daughter, Magma. Whereas Ocean, who was a bit wet by all accounts, has drifted away and is spending more time circulating with her new friend Eddy.

However, as is common in these messy family affairs there is a child involved, a troublesome sickly son by the name of Hydrothermal, who is caught between the warring factions. He does not like staying with his fractious father, who insists that he stays within strict boundaries that makes him hot under the collar so at every opportunity he escapes to be with his mother. Ocean's more Bohemian and turbulent lifestyle suits Hydrothermal much better and he enjoys mixing with Ocean's cool friends and tripping on whatever is the current high.

His father is cracking up under the strain. Hydrothermal has taken up smoking and things are looking black. However, Crust lives in hope that there will be some alteration and if the deposits come good, he and Mantle will have the opportunity to restrain Hydrothermal and heal some faults. When Crust suggests this to Ocean she just laughs out load “He-He-He:He-He-He-He” and mockingly calls him a plum pudding or worse, an infinite onion. Crust is left staring into the Abyss, Ocean's rebuff is the last straw so he decides to isolate himself and Mantle forever under an ever thickening muddy blanket and start the slow trek to eventual subduction.

Constraining the evolving volatile and melt geochemistry of magma reservoirs using apatite

Humphreys, M.C.S.[1], Stock, M.J.[2], Riker, J.[1,3], Smith, V.C.[2] & Brooker, R.[3]

[1]Durham University; [2]University of Oxford; [3]University of Bristol

Academic Staff 58

Magma evolution at subduction zones involves progressive fractionation of volatile-bearing magmas in the deep to mid-crust, followed by ascent and further differentiation in shallow crustal storage regions. The deeper fractionation may involve crystallisation from volatile-undersaturated magmas, whereas upper crustal magma storage is commonly linked to volatile saturation and active degassing. Methods to evaluate trace element and volatile variability in hydrous arc magmas are therefore critical to understanding the magmatic architecture in subduction zones.

We use the compositional record preserved in apatite to assess variations in melt and volatile geochemistry during magma storage and differentiation. Apatite is present in many magmas as microphenocrysts or as inclusions within phenocrysts, and can therefore preserve a temporal record of changing magmatic volatile contents in the lead-up to eruptions. New experiments and direct analysis of all the major volatile components (including C and OH) shows that apatite contains high CO_3^{2-} abundances and may therefore prove a sensitive tracer of pre-eruptive magmatic CO_2 contents. Modelling suggests that apatite volatile compositions are particularly sensitive to the onset of volatile saturation in magmas, which is a great advantage over melt inclusion studies. Results from Campi Flegrei (Italy) show that volatile saturation occurred very late during magma storage and may even have triggered eruptions due to pressurisation of the magma reservoir. Conversely, volatile saturation at Laacher See (Germany) occurred early, during growth of the crystal load. Apatite chemistry therefore represents a useful new tool for investigating temporal variations in magmatic volatiles prior to eruption.

Observations on gender equality within Durham's Department of Earth Sciences

Imber, J., Allen, M., Chamberlain, K., Foulger, G., Gregory, E., Hoult, J., Macpherson, C. & Winship, S.

Academic Staff 59

The progress of women to senior positions within UK higher education institutes has been slow. Women are worst represented in science, engineering and technology disciplines, where, in 2011, only 15% of professors were female. The national position is reflected in the Department of Earth Sciences at Durham University. The Department's gender profile shows steadily increasing proportions of females from undergraduate (ca. 38%) to postgraduate (ca. 42%) to postdoctoral (ca. 45%) levels, before dropping sharply with increasing seniority to 33% (n=1), 14% (n=1), 14% (n=1) and 13% (n=2), respectively, of lecturers, senior lecturers, readers and professors. The data suggest there is no shortage of talented female postgraduates and postdoctoral researchers; however, females are not applying, not being shortlisted, or not being appointed to academic roles in the expected proportions.

The Department's long term goal is fairness of opportunity for all, with a gender balance amongst academic staff that reflects the balance at postgraduate and postdoctoral levels. Our strategy is to attract greater numbers of high quality female applicants to academic positions, by making the application process more transparent, and by promoting positive cultural changes at all levels within the Department. As an example, we have recently introduced a mentoring scheme for postdoctoral staff, and plan to extend the scheme to academic staff. Nevertheless, we are conscious that achieving a representative gender balance amongst academic colleagues will take many years, based on historic staff turnover rates, and that lasting cultural change can be difficult to achieve.

Natural hydraulic fractures and the mechanical stratigraphy of shale-dominated strata

Imber, J., Armstrong, H., Atar, E., Clancy, S., Daniels, S., Grattage, J., Herringshaw, L., Trabucho-Alexandre, J., Warren, C., Wille, J. & Yahaya, L.

Academic Staff 60

The aim of this poster is to investigate stratigraphic variations in the spatial distribution and density of natural hydraulic and other fractures within oil mature, shale-dominated strata from the Cleveland Basin, northeast England. Median fracture densities recorded within the Cleveland Ironstone Formation are higher in ironstone beds (<2.1m-1) compared with shales (<0.9m-1). A qualitatively similar pattern occurs within the Whitby Mudstone Formation. However, the absolute values of median fracture density within different members of the Whitby Mudstone Formation range from 2.2–4.3m-1. Semi-quantitative estimates of the mineralogical "brittleness index" suggest the highly fractured, clay-rich Mulgrave Shale Member of the Whitby Mudstone Formation has a low brittleness. Our results are therefore inconsistent with the widely held assumption that natural fracture density is greatest within units characterised by a high brittleness index.

We propose that stratigraphic variations in fracture densities are more likely to result from the different distributions of crack driving stresses; formations containing decimetre-scale, and most likely stiff, carbonate layers (such as the Cleveland Ironstone Formation) will have differing crack driving stresses compared with silt- and mudstone dominated successions (such as the Whitby Mudstone Formation). The high fracture density observed within the Mulgrave Shale Member is also consistent with propagation of natural hydraulic fractures driven by fluid overpressure caused by maturation of organic matter concentrated within this unit. The next step is to investigate the relative importance of

maturation-driven overpressure v. mechanical heterogeneity by analysing the stratigraphic variations in fracture density within the underlying, organic-matter lean Redcar Mudstone Formation.

The East Australian, Tasmantid, and Lord Howe Volcanic Chains: Possible mechanisms behind a trio of hotspot trails

Kalnins, L.M., Cohen, B.E., Fitton, J.G., Mark, D.F., Richards, F.D. & Barfod, D.N.
Academic Staff 61

The east Australian and Tasman Sea region is home to a unique example of intraplate volcanism: three long-lived, sub-parallel volcanic chains spaced only about 500km apart. Here we present new $^{40}Ar/^{39}Ar$ results from the centre chain, the Tasmantid Seamounts, and show that the chain is strongly age-progressive, with an excellent correspondence to the age of the continental East Australian Volcanic Chain to the west and to the more limited ages available for the Lord Howe Seamount Chain to the east. Results from the Louisiade Plateau at the northern end of the Tasmantid Chain suggest that it is composed of basalts of the correct age to be a large igneous province associated with the initiation of the volcanic chain. How does such a unique trio of volcanic chains form? The clear age progression, long lifespan, and tie to the Louisiade Plateau are considered classic indicators of deep-seated plumes, but it is difficult to explain how three separate plumes could remain stable for over 30Ma when separated by little more than the radii of plume conduits. Here we examine alternative possible explanations for this volcanic pattern, including small plumes rising from a single deep-seated plume pooling at the 660km discontinuity, a single upwelling splitting around a subducting slab fragment, and small-scale convection triggered by topography on the lithosphere-asthenosphere boundary.

Formation and Maintenance of a Viscous Plug in a Strombolian Volcanic Conduit

Llewellin, E.W., Jenkins, A.P. & Jones, T.J.
Academic Staff 62

Textural studies of pyroclasts have shown that both degassed, crystal-rich magma, and gas-rich, crystal-poor magma may be ejected by a single strombolian explosion. Furthermore, some pyroclasts contain both magma types, intermingled. These pyroclasts have been interpreted as evidence of the presence of a plug of degassed, crystal-rich – and therefore high-viscosity – magma at the top of the volcanic conduit, overlying gas-rich, crystal-poor, low-viscosity magma. Analogue experiments have indicated that the presence of a viscous plug increases the vigour of strombolian explosions by enhancing the build-up of overpressure in the gas slug that drives them. The purported plug material has a higher density, as well as a higher viscosity, than the magma that underlies it. Consequently, the configuration is expected to be unstable, and the plug and underlying magma should convectively overturn. Does this mean that a viscous plug is an ephemeral feature? Or can a plug persist for long periods as a dynamic feature, which is continually created at the same rate at which it is convectively consumed? We conduct laboratory analogue experiments to investigate the formation and maintenance of a viscous plug. We drive thermal convection of a range of Newtonian and non-Newtonian magma analogue fluids in a 20cm diameter vertical pipe by heating the bottom, and cooling the top. The fluids have strongly temperature dependent rheology; both rheology and driving buoyancy are scaled to the volcanic scenario. We present preliminary results which characterize the spatial distribution of viscosity, density and velocity. We find that the hotter, lower-viscosity fluid ascends the core of the pipe, whilst the cooler, higher-viscosity fluid descends in an outer annulus. The upper region, in which the flow reverses direction, constitutes a dynamic plug.

Arclife – upper plate stress influences the sources of Sunda Arc magma

Macpherson, C.G., McCaffrey, K.J.W. & Pacey, A.
Academic Staff 63

Convergence is a prerequisite for the magmatic products that can be thought of as "arclife". And changing chemistry of magmatism is a feature of many plate margins that host arclife. Java's well established arc front is accompanied by distinct potassic stages through the history of its arclife. To determine the overarching controls, we explore if arc stress shapes the magmatic evolution that arclife signifies.

All the active volcanoes of central Sunda reflect an en echelon distribution of great circle segments, or lie on major lithospheric faults. Pacey et al (2013) interpreted this distribution, and its blurring further west near the Sumatran Fault, to result from magma channelling by upper plate stress. Arc segmentation also changes to the east, which coincides with (i) predominance of isolated, backarc, potassic volcanoes, (ii) near inactivity of what was, clearly, a substantial Pleistocene arc front, and (iii) Australian continental crust entering the subduction zone. This east Sunda arclife is interpreted as the collision with Australia changing stresses in the arc lithosphere and "choking" the Pleistocene arc system. Transport of low-degree, potassic partial melts was facilitated in the backarc as stress opened new magma pathways there. Central Sunda's arclife records the opposite chemical evolution with isolated, Plio-Pleistocene, backarc potassic volcanoes prior to the active, mainly tholeiitic, arc. This suggests that stress-induced weakness in central Sunda Arc lithosphere migrated towards the trench, consistent with forearc structures. Changes in magma supply and upper plate stress go hand-in-hand through the arclife of each part of the Sunda Arc.

How to Snowboard on Mars

McElwaine, J.
Academic Staff 64

Long, narrow grooves found on the slopes of martian sand dunes have been cited as evidence of liquid water via the hypothesis that melt-water initiated debris flows eroded channels and deposited lateral levées. However, this theory has several short-comings for explaining the observed morphology and activity of these linear gullies. We present an alternative hypothesis that is consistent with the observed morphology, location, and current activity: that blocks of carbon dioxide ice break from over-steepened cornices as sublimation processes destabilize the surface in the spring, and these blocks move downslope, carving out levéed grooves of relatively uniform width and forming terminal pits. To test this hypothesis, we describe experiments involving water and carbon dioxide blocks on terrestrial dunes and then compare results with the martian features. We present a theoretical model of the initiation of block motion due to sublimation and use this to quantitatively compare the expected behavior of blocks on the Earth and Mars. The model demonstrates that carbon dioxide blocks can be expected to move via our proposed mechanism on the Earth and Mars, and the experiments show that the motion of these blocks will naturally create the main morphological features of linear gullies seen on Mars. We include results on the latest fieldwork with the Discovery channel in May 2016.

Stresses, Porosity and Overpressure Modelling in Tectonic Regimes

Obradors-Prats, J.[1], Rouainia, M.[1], Aplin, A.C.[2] & Crook, A.J.L.[3]
[1]Newcastle University; [2]Durham University; [3]Three Cliffs Geomechanical Analysis, Swansea
Academic Staff 65

Pore pressure prediction in shales uses measured porosity-dependent rock properties in

conjunction with a Normal Compaction Trend (NCT), defined as the distribution of porosity with depth under hydrostatic conditions. The key assumption in 1D porosity-based pore pressure prediction is that mechanical compaction is driven by the vertical effective stress induced by the overburden. However, the approach is only valid in basins where disequilibrium compaction is the dominant overpressure generation mechanism. For basins subjected to tectonic deformation, the predictions made by 1D methods are likely to be deficient due to the impact of lateral stresses on compaction and overpressure generation.

We investigated these processes using a coupled fluid flow-geomechanical approach (ParaGEO finite element model) that accounts for the full 3D stress tensor. A plane strain model of a column was created with an initial geometry consisting of a clay layer 1 km wide and 0.4 km thick. We then performed a parametric study in order to investigate the influence of the sedimentation rate, the amount of shortening, the shortening rate and the post-tectonic burial on the predicted porosity and overpressure. The 2D models predicted an increase in overpressure of up to 16 MPa at 3.5 km depth and an additional porosity loss of up to 6 porosity units. Furthermore we used the model's output porosity to predict overpressure using a 1D porosity – effective stress approach. Compared to the 1D models, 2D models showed a maximum overpressure difference of 11 MPa at 3.5 km depth. These results indicate and quantify the importance of accounting for tectonic stress for both compaction and fluid pressure development.

Biocides in hydraulic fracturing: A comparison to agricultural and assessment of hazard and vulnerability with respect to groundwater pollution

Wilson, M.P.[1], Worrall, F.[2] & Davies, R.J.[1]

[1]Newcastle University; [2]Durham University

Academic Staff 66

Biocides are one possible chemical additive to frack fluids and their role is to control bacterial growth. Since biocides are designed to be toxic to particular organisms, their accidental or deliberate release into the environment has become a growing topic of concern, especially with regards to fracking. The objective of this study was to consider whether biocides proposed for use in fracking, could be a threat to English groundwater based on past groundwater monitoring data.

The study considered all groundwater samples analysed for biocides in English groundwater between 2005 and 2014. The monitoring records were compared to: records of application (both amount and area); and chemical and molecular data for the biocides. The study did not use traditional adsorption and degradation data as these parameters are prone to variability and are not pure molecular parameters.

The study showed that of the 110 biocides tested for in English groundwaters in the decade 2005 – 2014. The total number of detections was 2,234 out of 1475000 observations of 95 compounds, and 38 were compounds that were not applied during the period of record. The detection of these 38 compounds did not decline over the 10 year period implying very long residence times and that once compounds do pollute an aquifer, then they will be a persistent problem. Furthermore, the solubility of the range of biocides used in frack fluids would imply a potentially higher hazard than for most agricultural biocides, but molecular modelling implied that one compound could be safer than others.

The flux of organic matter through a peatland ecosystem – evidence from thermogravimetric analysis

Worrall, F.[1], Moody, C.S.[1] & Clay, G.D.[2]

[1]Durham University; [2]University of Manchester

Academic Staff 67

Carbon budgets of peatlands are now common and studies have considered nitrogen, oxygen and energy budgets, but no study has considered the whole composition of the organic matter as it transfers through a peatland. Organic matter samples were taken from each organic matter reservoir and fluvial transfer pathway and analysed the samples by thermogravimetric analysis. The samples analysed were: aboveground, belowground, heather, mosses and sedges, litter layer, a peat core, and monthly samples of particulate and dissolved organic matter. All organic matter samples were taken from a 100% peat catchment within Moor House National Nature Reserve in the North Pennines, UK, and collected samples were compared to standards of lignin, cellulose, humic acid and plant protein.

Results showed that the thermogravimetric trace of the sampled organic matter were distinctive with the DOM traces being marked out by very low thermal stability relative other organic matter types. The peat profile shows a significant trend with depth from vegetation- to lignin-like composition. When all traces are weighted according to the observed dry matter and carbon budgets for the catchment then it is possible to judge what has been lost in the transition through and into the ecosystem. By plotting this "lost" trace it possible to assess its composition which is either 97% cellulose and 3% humic acid or 92% and 8% lignin. This has important implications for what controls the organic matter balance of peatlands and it suggests that the oxidation state (OR) of peatland is less than 1.

ERC equipoise

ERC Equipoise is an independent Reservoir Evaluation company, specialising in all areas of upstream analysis. We offer a variety of services from independent reserve audits, to expert witness testimonials, to technical reservoir consulting including geophysical and geological modeling and reservoir simulation. With offices in London, Dubai and Singapore, ERC Equipoise provides consulting services for an international client base, analysing assets spanning the globe. Our team is made up of Professional Engineers, Geophysicists, Geologists and associated experts with experience in operations, consulting, academia and investment banking.

ERC Equipoise offers a wide range of advisory and technical services for clients, all focused on Reservoir Evaluation. Our experience in selecting the appropriate tools for the project, and our ability to draw upon our associated professionals and companies ensures that ERC Equipoise provides high standard work. Our Reservoir Evaluation Services comprise: Exploration and Appraisal, Field Simulation, Development and management, Valuation and Equity, Depth Modelling uncertainty, Seismic Processing and Modelling, Data services and Software development.

We work closely with Earth Sciences Department at Durham University as a member of the CeREES board, providing careers advice and internships for students, supporting Conferences and also actively looking to recruit students. We also teach a practical course to the undergraduates.

United Kingdom Office
ERC Equipoise Limited
6th Floor Stephenson House
2 Cherry Orchard Road
UK
CRO 6BA

+44 (0) 20 8256 1150
info @ercequipoise.com
www.ercequipoise.com

Singapore Office
ERC Equipoise Pte Ltd
205 North Bridge Road
#14-01 Raffles City Tower
Singapore 179101

+65 6331 5161

Programme Summary

Posters/Lunch

Hydrocarbons

Environmental

Geodynamics, Volcanology and Structural Geology

	TR 3
09:15-09:30	Adrian Saw
09:30-09:45	William Thorogood
09:45-10:00	Matthaeos Volikas
10:00-10:15	Harry Brooksbank
10:15-10:30	James Phillips
10:30-11:00	**Coffee**
11:00-11:15	Siobhan Roze
11:15-11:30	Jamie Alderson
11:30-11:45	Andrew Wakefield
11:45-12:00	Rosemary Davies
12:00-12:15	Erica Powell
12:15-12:30	
12:30-14:00	**Poster Session I/Lunch**
14:00-14:15	Anna Kenton
14:15-14:30	David Riley
14:30-14:45	Daniel Stephen
14:45-15:00	Chris Malliband
15:00-15:15	Katharine Groves
15:15-15:30	Ryan O'Hare
15:30-17:00	**Poster Session II/Drinks**

With thanks to our supporters: